Micro-UAS as a tool for observing the Arctic Environment

Gijs de Boer[1,2] (gijs.deboer@colorado.edu), John Cassano[1], Dale Lawrence[1]

(1) The University of Colorado – Boulder
(2) NOAA Earth System Research Laboratory, Physical Sciences Division

Unmanned aircraft systems (UAS) are rapidly becoming a popular tool for scientific measurement of the atmosphere, cryosphere, oceans, and Earth surface. The ability to obtain high-resolution, *in-situ* and remotely sensed datasets without the need for large, expensive manned research aircraft is attractive to scientists across disciplines. In this statement we outline current work on use of "micro" UAS (mUAS) at high latitudes, including information on platforms, recent campaigns, current limitations, regulatory issues and future directions.

Currently the US Federal Aviation Administration (FAA) considers platforms lighter than 55 lbs. as small UAS (sUAS). Within this framework also lies the mUAS category, consisting of platforms with a net weight under 4.4 lbs. These mUAS platforms generally offer a very low-cost platform from which to base measurement operations. Included in this category are the DataHawk (Lawrence and Balsley, 2013) and SUMO (Reuder et al., 2009) UAS. The DataHawk was originally developed at the Unviersity of Colorado – Boulder by Professor Dale Lawrence, and has a ~1.2 m wingspan, a total weight of ~1kg, and a total parts cost of around $950. The SUMO is a modified version of the commercially available Multiplex Funjet, with a wingspan of 0.8 m, a total weight of 580 g and an approximate cost of $5000. These platforms are quite flexible in what quantities they measure, and require very limited infrastructure for operations. Flights generally involve two people, including one pilot and one observer, a laptop ground station, an antenna, and a bungee launcher. Both platforms can be hand-launched, either by throwing the aircraft or using a bungee launcher system. Navigation can be fully autonomous using onboard autopilot systems programmable from the surface both before and during flight. The low cost of these platforms makes them perfect candidates for high-risk operations, where successful recovery of the aircraft is not necessarily guaranteed.

At present, the regulatory bodies of the airspace in which operations take place govern use of these platforms. The Arctic airspace is divided into several different Flight Information Regions (FIRs), overseen by the USA, Canada, Russia, Norway, and Iceland. In the US Arctic the FAA prohibits commercial (including research) use of UAS of any size without authorization through the certificate of authorization (COA) or other exemption pathways. However, several groups have been able to operate in coastal Alaska, either by successfully securing a COA, flying in areas of restricted airspace, or by flying in international waters using "due regard" (definition?). Certain agencies, such as the US Department of Energy (DOE) have provided leadership in the use of UAS in the US Arctic by providing complementary ground-based observational facilities in areas of previously established restricted airspace (e.g. Oliktok Point, Alaska) and by engaging the FAA to find new opportunities for use of UAS, including the newly formed "Warning Area" (W-220) extending from the Alaskan shoreline to 82° N latitude.

Under these provisions, several campaigns using mUAS have been carried out in recent years in the US Arctic and beyond. In the summer of 2013, the interagency Marginal Ice

Figure 1: The DataHawk mUAS making measurements of the lower troposphere over Oliktok Point, Alaska.

Zone Experiment (MIZOPEX) included operation of the DataHawk mUAS from Olitkok Point. For this campaign, the DataHawk was configured as a “Self-Deployable Surface Sensor” (SDSS), carrying a thermistor string to provide information on upper ocean (10 m) temperature for an extended time period. In October of 2014, the DataHawk went back to Oliktok Point to make measurements of atmospheric temperature, humidity and winds during the fall freeze up of near-shore ice. Flights were conducted over a two-week period at very low altitudes (10 m) to evaluate variability of atmospheric conditions over various and changing surface types. Most recently (August, 2015), an updated version of the DataHawk was deployed to Oliktok Point as part of the DOE-funded “Evaluation of Routine Atmospheric Sounding Measurements” (ERASMUS) campaign. During this campaign, the aircraft was used as a recoverable radiosonde, providing frequent, regular profiles of atmospheric temperature and humidity in the lower troposphere over a two-week period. The SUMO was used in a similar manner during a two-week field campaign on the Ross Ice Shelf, Antarctica during January 2014.

At the current time, there are some drawbacks to using these systems for research. First, the small stature and limited power of these aircraft limit the atmospheric conditions in which they can operate. Most noticeably, mUAS are hindered by winds greater than ~15 m s^{-1} and by any sort of icing conditions, since they cannot carry active de-icing equipment. In addition, there is limited availability of commercial sensors small enough to fit on these micro-scale platforms. Where sensors do exist, their performance, in the form of accuracy, response time, or otherwise, is often insufficient for providing the high-quality measurements necessary for scientific applications (e.g. Cassano 2014). While the research community has begun to develop their own instrument options, the accuracy of these research instruments is generally poorly characterized, and extensive testing of instrumentation is necessary to advance the scientific use of these platforms in the future. However, with ongoing characterization of instrumentation, these platforms will continue to be an invaluable asset for the Arctic observing community, providing previously unattainable measurements of the high-latitude environment at a relatively low-cost.

References:

Cassano, J.J. 2014: Observations of atmospheric boundary layer temperature profiles with a small unmanned aerial vehicle. *Antarctic Science*, **26**, 205-213. DOI 10.1017/S0954102013000539

Lawrence D.A. and Balsley, B.B. 2013. High-Resolution Atmospheric Sensing of Multiple Atmospheric Variables Using the DataHawk Small Airborne Measurement System. *J. Atmos. Oceanic Technol.*, **30**, 2352–2366. doi: http://dx.doi.org/10.1175/JTECH-D-12-00089.1.

Reuder, J., Brisset, P., Jonassen, M., Muller, M. and Mayer, S. 2009: The Small Unmanned Meteorological Observer SUMO: A new tool for atmospheric boundary layer research. *Meteor. Zeitschrift*, **18**, 141-147. DOI 10.1127/0941-2948/2009/0363

Adjoint Sensitivity Analysis and Observing System Simulation Experiments as an tool to analyze and optimize observations in the Arctic Ocean

Gleb Panteleev[1], Max Yaremchuk[2], Jacob Stroh[1], Oceana Francis[3], Pamela Posey[2], David Herbert[2]
(1)-International Arctic Research Center, UAF, Alaska,(2)-Naval Research Laboratory, Mississippi;
(3)- University of Hawaii, Hawaii.

Abstract Efficient Ocean Observational System in the Arctic Ocean is critical for understanding of the environmental changes in the Arctic where data acquisition is extremely complicated and expensive. Adjoint Sensitivity Analysis (ASA) and Observing System Simulation Experiments (OSSE) are the powerful tools that could be used for the optimization of the existing and incoming observational programs in the Arctic Ocean. We provide two examples how the ASA and OSSE can be used for optimizing the locations of the High Frequency Radars and passive tracer survey.

Introduction

With the diminishing of sea-ice during the past decades, we observe significant changes of the hydrophysical conditions in the Arctic Ocean. An incomplete list of observed changes includes: intensification of warm Pacific Water inflow through the Bering Strait (BS) (*Woodgate et al.,* 2012), changes in freshwater (FW) balance in the BS and in the Eurasian Basin, enhanced Arctic oscillation (AO) index “due to cyclonic shift in the ocean pathways of Eurasian runoff forced by strengthening of the west-to-east Northern Hemisphere atmospheric circulation” (*Morison et al.*, 2012), amplification of regional significant wave height by 35% (*Francis et al.*, 2010), and development of a new role for sea waves to further diminish Arctic sea-ice (*Simmonds and Rudeva*, 2012) and enhance vertical mixing *(Qiao et al.*, 2004). There is also a significant increase of human activity in the Arctic Ocean, which includes trans-Arctic transportation and shipping, mineral extraction, and oil/gas exploration in the Arctic shelf. These activities risk additional impacts on the fragile Arctic ecosystem.

Because of these changes and increased risk of accidents and technological disasters, there is a strong need for an efficient Observational Network (ON) that would: allow for reliable estimation of the observed changes; explain the most important factors responsible for the changes; forecast future changes in the Arctic Ocean hydrophysical, hydrochemical, and ecological states; and aid in responding to undesirable events. The need for better understanding has resulted in several observational initiatives such as Nansen/Amundsen Basin Observing System (NABOS), Beaufort Gyre Exploration Project (BGEP), East Siberian Shelf Study (ESSS), Distributed Biological Observatory (DBO), deployment of high frequency radar (HFR) systems along the Alaskan Coast, and other such programs.

Essential elements of modern observations in the Arctic Ocean include velocity observations from moorings and coastal High Frequency Radars (HFRs), and hydrographical observations from ships. Currently there are a significant number of moorings deployed in the Pacific side of the Arctic Ocean in the frame of the multinational efforts. However, such observational plans are usually based on qualitative understanding of the investigated processes and/or scientific intuition, both of which may be at least sub-optimal or subjective.

An ideal ON plan should be guided by an objective strategy that optimizes the expenses of monitoring coastal circulation in the context of existing activity and existing needs. A prerequisite for developing such a strategy is the ability to answer the following questions:

- How many observations do we need in order to obtain reliable estimates of various target quantities (TQs) (such as transports through certain sections, surface circulation) in these regions? Further: what is the relative impact of additional observations?

-What are optimal locations for glider-based scanning, mooring deployment, and HFR installation? What is optimal combination between these instruments?

-How do observations in one region (*e.g.* velocity observations at particular sites in the Chukchi Sea) correlate with observations in another region (*e.g.* with observation in the Bering Strait)?

- In what regions do we need improved coverage and what are the requirements for observational accuracy?

Given the high expense observational instrumentation and deployment logistics in the Arctic region, the first step in ON development should be preliminary analysis and optimization of future plans. For example, when located in appropriate sites along the Alaska coastline, HFRs can be effectively used to support local marine transportation and offshore operations, *i.e.* to provide benefit to local communities and businesses. Simultaneously, these data can contribute to numerous scientific projects of climatological importance, such as monitoring of the Bering Strait transport and the Alaska Coastal Currents.

Tools for objective planning of observation systems are well known and include the Adjoint Sensitivity Analysis (ASA) and Observing System Simulation Experiments (OSSEs). They are widely applied for analysis and planning of the observational grid in operational meteorology, where the corresponding volume of observations is critical for accurate weather forecast (Errico et al., 2013, Lahoz et al., 2005, Timmermans et al., 2015). Over the past decades, there have also been persistent efforts to introduce a similar approach for ocean observational programs. Despite these attempts, observational planning of oceanographic surveys and long-term monitoring still do not usually include quantitative estimates of the efficiency of the proposed observational plans.

In this paper, we describe the basic ideas behind the ASA and OSSEs techniques, and show how application of these tools may help to optimize the location of the HFRs, identify the gaps in existing observational programs. and increase the information content of the various passive-tracer observations collected during ship surveys.

2. Approaches

Currently, there exist two well-established techniques for optimizing ONs. Both of them make extensive use of link between numerical models and observations, and may be used in sequence.

First, one would perform Observing System Simulation Experiments (OSSEs) in order to identify optimal *in situ* observing site locations, the required measurement frequency, and acceptable levels of uncertainty. The idea underlying OSSEs is to simulate “data” using some reference model solution as a “true ocean state”, contaminate these data with noise (mimicking observational and modeling errors), and then reconstruct the “'true state”' from these “data.” The ancestor of the OSSE approach is the well-known twin-data experiment procedure, which is a basic method of testing data assimilation schemes developed during the last couple of decades.

Second, one analyzes the dynamically-induced correlations between the any TQs and observations through Adjoint Sensitivity Analysis (ASA) (*Köhl and Stammer,* 2004, *Panteleev et al.*, 2008). This approach requires the use of tangent linear and adjoint models (*Marchuk*, 1995; *Wunsch,* 1996), which may be problematic for some models and require time-consuming development if they are not already available.

3. Optimal location of HFR

The difference between these approaches is that ASA is usually applied to the states previously optimized with respect to available data, whereas the statistical analysis of OSSEs is usually applied to non-optimized model solutions, which may differ significantly from the true state of the ocean. The ASA is based on the strong relationship between observations and model state, which is the basic advantage of the 4-dimensional variational data assimilation approach based on the tangent linear and adjoint modeling. The technique allows one to analyze the impact of any additional observations on the optimized model state, and then project this to any TQ of interest. These steps are formally described as applications of linear operations on the model state and the reverse algorithm is also possible and usually less expensive.

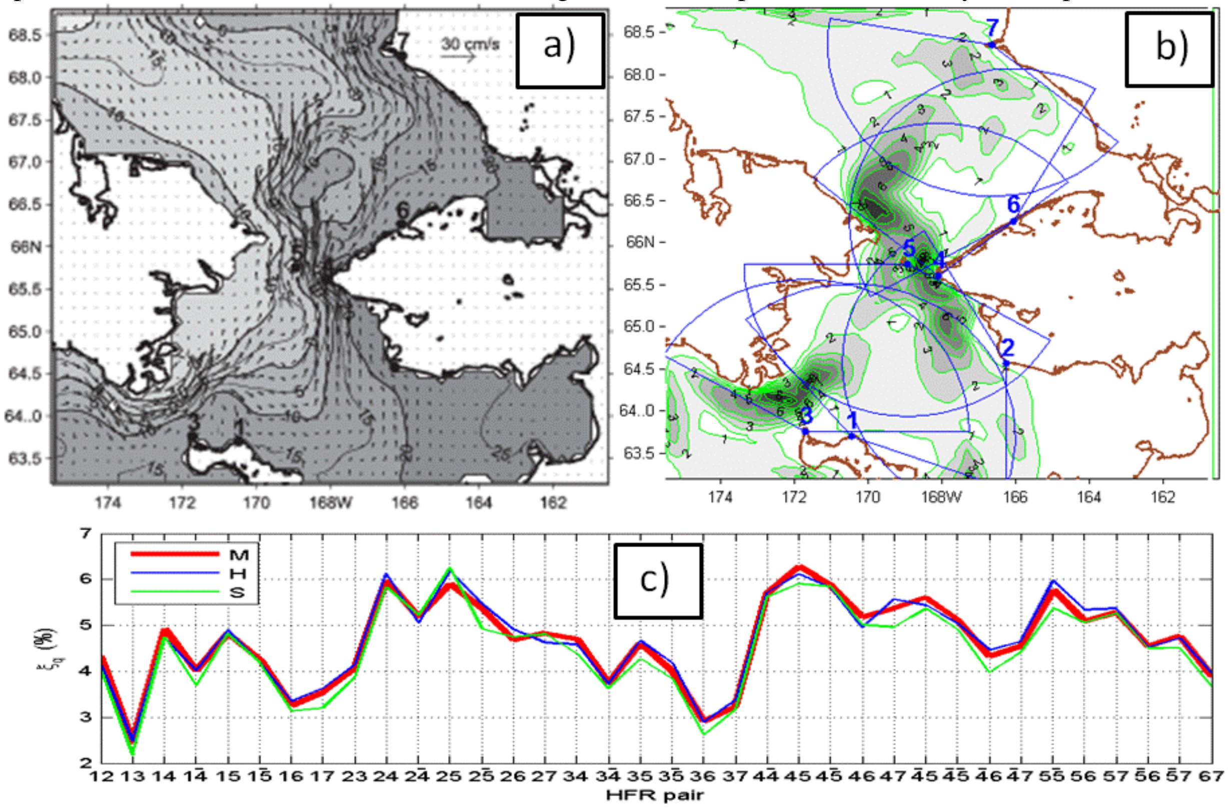

Figure 1. **a)** Surface current and SSH in the BS region. **b)** Time-averaged map of the mean BST sensitivity to surface velocity observations. Sensitivity values are normalized by their maximum at the Bering Strait. Number 1--7 designate the possible sites for HFR near villages along the Alaska coast: Savonga (1), Sinuk (2), Gambel (3), Wales (4), Diomede (5), Shishmaref (6) and Point Hope (7). **c)** Relative reduction of the errors in estimation of the momentum (M), heat (H), and salt (S) transports through the strait for various pairs of HFRs. Numbers labeling HFR pairs correspond to locations in Fig.1b. Bars over Wales (point 4) and Diomede (point 5) locations denote northward-looking antennas at those sites.

The key result of an ASA is an adjoint sensitivity map which establishes a formal relationship between the TQ and all elements of the model state. Figure 1b shows a time-averaged ASA map of the mean Bering Strait transport (BST) sensitivity to the surface velocity observations for the case of a slowly varied summer climatological circulation shown in Fig.1a (*Panteleev et al.*, 2015). Roughly speaking, the map in Fig.1b says that total flows through the Bering Strait are most strongly correlated with (observed) velocity values in the areas of maximum sensitivity, so that the HFR pair ‘45’ (Diomede and Wales, Fig. 1c) best measures the TQs of mass, heat, and salt (MHS) transport through the strait. An immediate conclusion is that if we have one mooring and want to measure the Bering Strait transport, it should be deployed in the American Part of the Bering Strait. Planning the deployment of multiple moorings would require a more complicated analysis taking into account adaptive sampling strategy (Bishop et al., 2001, Daescu and Navon, 2004), or conduct multiple OSSEs as in Panteleev *et al*. (2013a).

HFRs observe surface velocity on the rays which project radially outward from the antenna with radius of about 200--250km (Fig. 2b). Therefore, it is necessary to account for the more complicated “observational operator” corresponding to the HFR configuration. This operator takes into account the area covered by the HFR observations as well as spatial orientation of the rays along which the measurements occur. Further, it must account for the decreasing accuracy of HFR observations with distance from the antenna; observations near the HFR site are usually more accurate than those further away. Technical details for construction of the HFR observation operator and error covariance approximation can be found in Panteleev *et al.* (2015).

By applying simple algorithms that take into account the geographical location of different HFRs on the adjoint sensitivity map Fig.1b, we can easily estimate the reduction of the Bering Strait transport errors due to observation by any pairs of the HFR as well as estimate the efficiency of those pairs. In particular, Fig.2c shows that two HFR located in Diomede and Wales (pair '45') and looking south will provide the least estimation error of the Bering Strait transport. The other reasonable combinations are HFR installations in Sinuk and Wales (pair '24'), Sinuk and Diomede (pair '25'), and two HFR in Wales looking to the north and south. Taking into account that installation in Diomede is logistically complicated (T. Weingartner, *personal communication*), the HFR configurations at Sinuk-Wales and Wales-Wales are reasonable sub-optimal alternatives to the Diomede-Wales setup. Note, however, that deployment at Wales-Wales maybe significantly cheaper.

The economical constrains may be technically incorporated into the algorithm, so in practice, the Wales-Wales pair can be found as a "best" solution when logistical expenses of installation and maintenance are included in the optimization. Simultaneously considering both financial and scientific (Bering Strait transport) values requires a relative weighting of these factors. This introduces subjectivity into the process, and it is therefore reasonable to avoid the economic aspects when pursuing an objective analysis.

The outlined algorithm can be easily extended to optimize installation locations and analyze ON efficiency for more than two HFR. In addition, we can conduct the multiple OSSEs and validate the results inferred from the adjoint sensitivity maps and other by-products of the ASA technique (*e.g. Panteleev et al.*, 2008, 2015). A very high number of moorings and/possible sites for deployment requires running the many OSSEs, which can be computationally prohibitive.

4. Optimal passive tracer survey

The ASA technique is a sensitivity analysis, which is formally involves computation of the TQs' derivatives (such as the MHS transports above) with respect to observations. This requires differentiability of the observation operator, so the ASA appraoch can only apply to certain kinds of observation systems. In the case of a non-differentiable observational operators, OSSEs are probably the only way to optimize ONs. An important example giving rise to non-differentiable observational operators are passive tracer surveys, the method of observation typically used in the study of the Arctic Ocean ecosystem.

The list of the publication related to optimal hydrographic surveys has a long history (*e.g. Panteleev and Semenov*, 1988; *Beckers and Rixen* , 2003). Here we present a simple example how the OSSE technique may help to optimize observations of passive tracers in the Chukchi Sea, where intense and variable currents should be taken into account for planning the surveys. The approach is based on a four-dimensional variational (4Dvar) algorithm applied to an advection-diffusion differential equation describing the behavior of passive biological content (such as small larvae, fish eggs, *etc.*) in known velocity field. The approach was successfully used to reconstruct silicate, phosphate, and nitrates concentrations in the Bering Sea (*Panteleev et al.*, 2013b).

To illustrate the approach, we utilize synthetic data sets which idealize those obtained from biological surveys in the Chukchi Sea. The background velocity field is a realistic reconstruction for the same region during August-September, 2012 as obtained using 4Dvar data assimilation with 10 km resolution. The mean Sep 1--3, 2012 circulation and mean "true" distribution of the passive tracer are shown at Fig.2a,b. A conventional passive tracer survey in the southern Chukchi Sea lasts approximately 3 days, during which tracer observations occur along the ship path. There are multiple possible sample paths for the survey, a few of which are shown by blue traces in Fig.2b,c,d. Each path yields a different set of tracer observations since this TQ moves with the background velocity field. To analyze the efficiency of different surveys, we sample the "true" passive tracer along the proposed cruise tracks with a relative measurement error of 10%.

Using the 4Dvar data assimilation algorithm applied to the advection-diffusion tracer model, the passive tracer field is reconstructed from observations taken along the different survey paths. The root-mean-squared difference between reconstructed and "true" distributions of the passive tracer is used as a metric to evaluate the efficiency of different surveys. Fig.2c,d shows that the ship paths (which define the survey observational operators) have a strong impact on the tracer field reconstruction, and an appropriate path may decrease the RMS by 10--20% and thereby reconstruct the tracer more accurately. Fig.2e,f show reconstructions obtained from the same ship paths shown in Fig.2c,d using traditional linear interpolation methods which do not account for advection of passive tracers. This method is common in analysis of the hydrochemical and biological observations. Comparing Fig.2c,d with Fig.2e,f shows that use of the non-stationary 4Dvar assimilation method is more important than the survey path configuration, and typically decreases the reconstruction RMS error by 20--35% as compared to non-stationary interpolation algorithms.

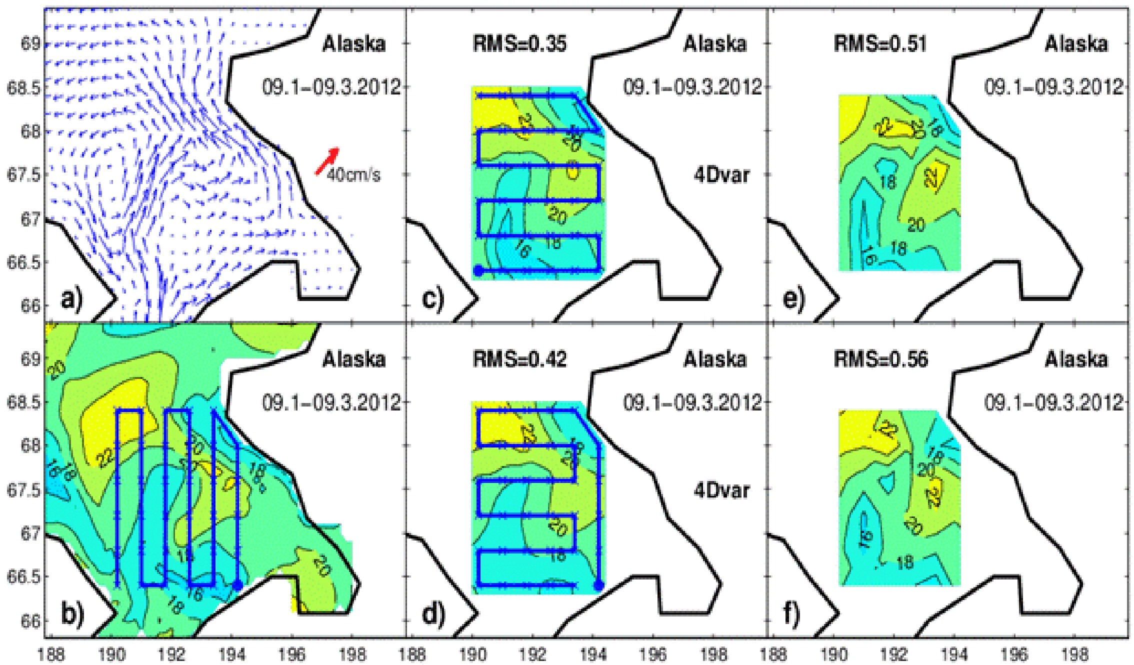

Figure 2. Mean circulation **(a)** and idealized passive tracer distribution **(b)** in the Southern Chukchi Sea during Sep 1--3, 2012. Blue lines designate the observation locations along the ship path. **c),d)** Results of the 4Dvar reconstruction of the passive tracer using observations from the overlain ship path. **e),f)** Results using the same paths but obtained using the linear interpolation algorithm.

4. Conclusions

The ASA and OSSE algorithms have been successfully used by agencies such as the National Aeronautics and Space Administration (NASA), NOAA, Meteo France, and the Met Office UK for planning and testing new observational systems in atmospheric science. Obviously they have a strong potential for the optimization of the observational programs in the in the Arctic Ocean. Currently, they can be easily applied for such planning using the existing (climatological or seasonal) circulations. Recently, we developed a prototype adjoint sensitivity web-server that can be used to optimize a set of user-specified HFR installations in the Southern Chukchi Sea (http://oregon.iarc.uaf.edu/hfr.html) using a non-stationary climatological summer circulation. We plan to develop a similar web-server for optimizing passive tracer surveys. However, these optimization systems and web-servers are designed for optimization with respect to regional *climatological* circulations. This is reasonable for long-term observation system planning (such as mooring deployment and HFR installation sites), but a practical survey optimization system would require an operational circulation model.

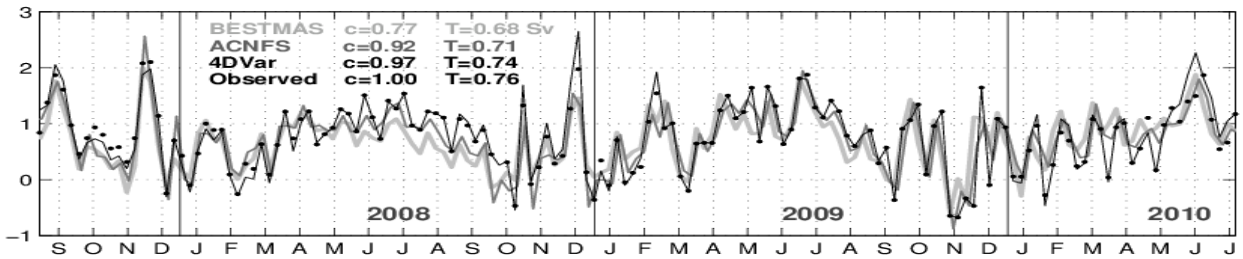

Figure 3. Weekly averaged Bering Strait transports (Sv) in the optimized solution (solid black line), and from the ACNFS (gray) and Bering Ecosystem Study ice-ocean Modeling and Assimilation System (BESTMAS) (light gray) output. Observed values are shown by solid dots. The time averaged values of the transport T and correlation coefficients c with observations are given.

Our analysis of the circulation from the Arctic Cap Forecast Nowcast System (ACFNS) developed in Naval Research Laboratory (http://www7320.nrlssc.navy.mil/hycomARC, *Posey et al.*, 2010) shows that ACFNS provides accurate estimates of the circulation in the southern Chukchi Sea. In particular, the Bering Strait transport from ACFNS has 0.92 correlation with observed volume transport (Fig.3). Flow though the Bering strait is the most influential forcing for the southern Chukchi Sea and thus, the velocity field from this system is recommended as a first guess state for different data assimilation algorithms, including the ones described above. Thus, access to operational output from the ACNFS would enable the development of online tools for operational survey optimization in the Chukchi Sea via OSSE and for post-processing of these observations using the simple advection-diffusion approach. Currently, we are pursuing the development of this kind of tool.

References:

Beckers, J.-M., and M. Rixen. 2003. "EOF Calculations and Data Filling from Incomplete Oceanographic Datasets." Journal of Atmospheric and Oceanic Technology 20.12

Bishop, G. et al., 2001."Adaptive Sampling with the Ensemble Transform Kalman Filter. Part I: Theoretical Aspects", 129,420-437 Montly Weather Review

Daescu D.N. and I.M. Navon, "Adaptive observations in the context of 4D-var data assimilation," Meteorology and Atmospheric Physics, vol. 85, no. 111, pp. 205–226, 2004.

Errico et al., 2013 Development and validation of observing-system simulation experiments at NASA's Global Modeling and Assimilation Office Quarterly Journal of the Royal Meteorological Society, 139-674, 1162–1178, Part A

Francis, O. et al. 2011. "Ocean wave conditions in the Chukchi Sea from satellite and in situ observations." Geophysical Research Letters 38.24

Köhl, A., Stammer, D., 2004. Optimal observations for variational data assimilation. J. Phys. Oceanogr. 34, 529

Lahoz et al. 2005. An observing system simulation experiment to evaluate the scientific merit of wind and ozone measurements from the future SWIFT instrument Q. J. R. Meteorol. Soc.,131, pp. 503–523 doi: 10.1256/qj.03.109

Marchuk, G., 1995. Adjoint Equations and Analysis of Complex Systems. Kluwer Academic Publishers.

Morison, J., et al. 2012. "Changing Arctic Ocean freshwater pathways." Nature 481.7379

Qiao, Fangli, et al. 2004. "Wave□induced mixing in the upper ocean: Distribution and application to a global ocean circulation model." Geophysical Research Letters 31.11

Panteleev, G., and E.V. Semenov. 1988. "On the strategy of hydrological array measurements." Oceanologia 6

Panteleev, G.G, M.Yaremchuk, D. Nechaev, 2008. “Optimization of mooring observations in Northern Bering Sea”, *Dynamics of Atmospheres and Oceans*, doi:10.1016/j.physletb.2003.10.071.

Panteleev, G., et al. 2010. "Reconstruction and analysis of the Chukchi Sea circulation in 1990–1991." Journal of Geophysical Research: Oceans 115.C8

Panteleev, G., et al., 2013a T.Kikuchi Configuring High Frequency Radar observations in the Southern Chukchi Sea, *Polar Science*, 7, 72-81, 2013.

Panteleev, G., et al. 2013b. "Seasonal climatologies of oxygen and phosphates in the Bering Sea reconstructed by variational data assimilation approach." Polar Science 7.3

Panteleev, G., et al. 2015. "Optimization of the high-frequency radar sites in the Bering Strait region." Journal of Atmospheric and Oceanic Technology 32.2

Posey, P., et al. 2010. "Validation of the 1/12 Arctic cap nowcast/forecast system (ACNFS)." EGU General Assembly Conference Abstracts. Vol. 12.

Simmonds, I., and I. Rudeva. 2012., The great Arctic cyclone of August 2012, Geophysical Research Letters 39

Timmermans et al., 2015. Observing System Simulation Experiments for air quality, Atmospheric Environment, 115, 199–213

Woodgate, R., et al. "Observed increases in Bering Strait oceanic fluxes from the Pacific to the Arctic from 2001 to 2011 and their impacts on the Arctic Ocean water column." Geophysical Research Letters 39.24 (2012).

Wunsch, C., 1996. The Ocean Circulation Inverse Problem. Cambridge University Press, Cambridge, UK

A White Paper for the Arctic Observing Summit Meeting,
March 2016, University of Alaska Fairbanks

Opportunities for Sustained Arctic Observations and Scientific Collaborations at the US Department of Energy Atmospheric Radiation Measurement (ARM) Facilities on the North Slope of Alaska

Jasper (Joe) Hardesty†, Mark Ivey, Dari Dexheimer, Fred Helsel, Dan Lucero
Sandia National Laboratories
†contact email: joharde@sandia.gov

Gijs de Boer, University of Colorado Boulder/CIRES (Cooperative Institute for Research in Environmental Sciences)

Sandia Report #SAND2015-9069 C
Sandia National Laboratories is a multi-program laboratory operated by Sandia Corporation, a wholly owned subsidiary of Lockheed Martin company, for the U.S. Department of Energy's National Nuclear Security Administration under contract DE-AC04-94AL85000.

Abstract

The U.S. Department of Energy Atmospheric Radiation Measurement (ARM) program has maintained facilities for observations on the North Slope of Alaska since 1997. With ARM sites at multiple NSA locations, these facilities provide measurements and resources to support research and field campaigns for a wide spectrum of users and partners. Observations of terrestrial, ocean and atmospheric systems using land based, remote and aerial equipment provide opportunities to solve problems and serve the growing community of researchers and stakeholders working in the Arctic. This paper describes the current facilities, recent activities, science objectives, developing capabilities, future plans and opportunities to expand ARM NSA contributions and collaborations.

Introduction

The U.S. Department of Energy (DOE), Office of Science/Biological and Environmental Research, Atmospheric Radiation Measurement (ARM) program provides scientific infrastructure and data to the international Arctic research community via atmospheric research facilities located on the North Slope of Alaska (NSA) (www.arm.gov/sites/nsa). An instrumented ARM facility was established on the coast of the Arctic Ocean near Barrow Alaska in 1997. A smaller inland facility was operated in Atqasuk between 1999 and 2010. This facility in Atqasuk included infrastructure that was used on the icebreaker-based Surface Heat Budget of the Arctic (SHEBA) campaign. SHEBA involved the deployment of an instrumented ice camp within the perennial Arctic Ocean ice pack that began in October 1997 and lasted for 12 months. In October of 2013, an ARM Mobile Facility (AMF3) was constructed at Oliktok Point, Alaska. Sandia National Laboratories manages and operates the ARM NSA facilities for DOE. Combined, these sites constitute the ARM NSA Megasite; a network of facilities to provide complementary high-density observations for improved understanding of arctic processes. The locations of Barrow, Oliktok Point and Atqasuk are shown in Figure 1.

Barrow is at the northernmost point in the US, 530 kilometers (330 miles) north of the Arctic Circle, and contains some of the most robust infrastructure on the North Slope. The Barrow ARM site benefits from this to provide consistent measurements from facilities that include instrumentation, lodging, communications and maintenance support. An extended range AERI (ER-AERI) built specifically for the high latitudes where low water vapor concentrations are common is operating at Barrow, and many instruments have been hardened to withstand temperatures that drop below (-)40 C/^{o}F.

The Oliktok Point site consists mainly of an aircraft hangar, gravel runway, instrumentation vans, and lodging that are located on the grounds of an active US Air Force facility (Oliktok Point Long Range Radar Site, LRRS). Restricted airspace R-2204 encompasses a 4.8 km (2 mile) radius centered on Oliktok Point and can be accessed from a gravel runway and pads at the LRRS. Warning Area W-220 extends approximately 1300 km (700 nautical miles (nm)) into international airspace and is approximately 75 km (40 nm) wide. The R-2204 and W-220 air spaces are illustrated in Figure 1. Unique among ARM facilities, it is the only ARM site with restricted airspace, providing opportunities for research with tethered balloons, unmanned aircraft systems, and modified manned aircraft, without the need for an FAA waiver. It is also the only ARM site located within the North Slope oilfields, and the only site hosted by the US Air Force. The proximity to the LRRS and to ongoing oil extraction activities provides Oliktok Point with amenities, infrastructure, and logistical services not readily found elsewhere in the Arctic.

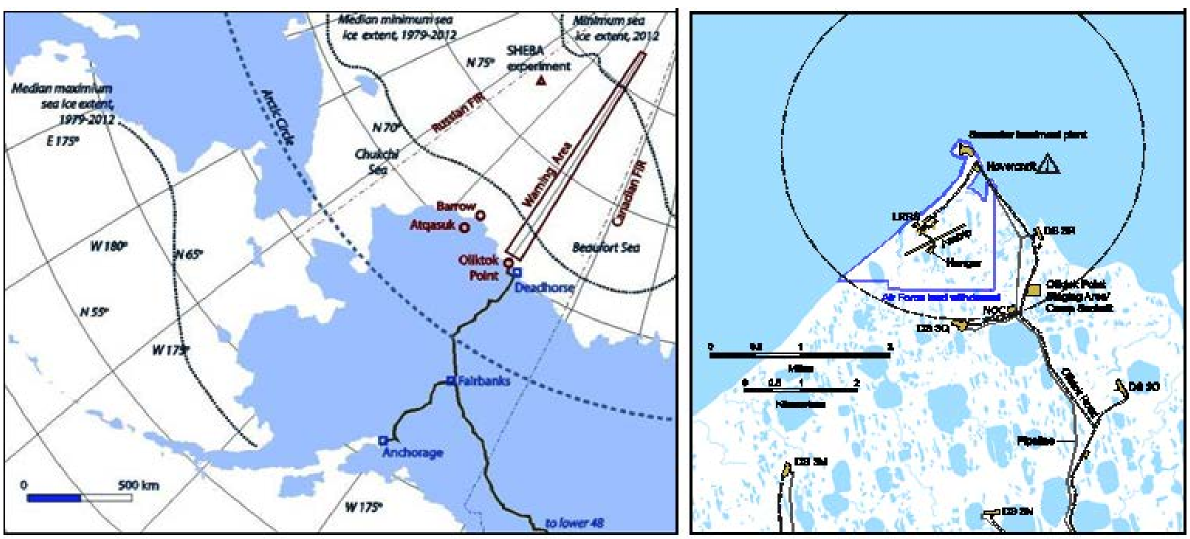

Figure 1: ARM North Slope Facilities and Controlled Air Spaces at Oliktok Point/AMF3. (**Left**) ARM facility sites (red circles) and W-220 international warning air space; (**Right**) Oliktok Point R-2204 restricted air space.

Instruments and Scientific Infrastructure at Barrow and Oliktok Point/AMF3

The mission of the ARM North Slope Alaska is to:

- Provide infrastructure support for climate research to the scientific community.
- Provide a broad range of data to help answer questions about Arctic climate change.
- AMF3 is gathering data using instruments that obtain continuous measurements of clouds, aerosols, precipitation, energy, and other meteorological variables.
- Provide climate data that is freely available to the international community through the ARM data archive.

The ARM NSA field campaigns and ongoing baseline measurements are conducted from the Barrow and Oliktok Point/AMF3 sites. Images of both sites are shown in Figure 2.

Figure 2: ARM North Slope Alaska Facilities. (**Above**) Barrow facilities are fixed, while (**Below**) Oliktok Point/AMF3 facilities are mobile.

Measurements at the Margins: Trends that point to accelerated warming in the Arctic include the shrinking spread and year-to-year loss of sea-ice and temperatures (rising at twice the rate of the rest of world), and increasing instability in the region's permafrost layer, which stores vast amounts of methane in its frozen grip—for now. Computer models used to test scientific theories have yet to simulate these conditions with a high level of accuracy. Largely due to the difficulties in obtaining the needed observational data for the models, the ARM NSA facilities collect data to fill those gaps. Instruments that are operated at these sites are listed in Table 1.

Table 1: Atmospheric Observation Instrumentation at ARM NSA Facilities

Barrow Site	Oliktok Point/AMF3
Atmospheric Profiling Instruments	
Automated Balloon-Borne Sounding System (SONDE)	Balloon-Borne Sounding System (SONDE)
Radar Wind Profiler (RWP)	Tether Balloon-Borne Sounding System (SONDE)
	Unmanned Aerial Systems (UAS)
Cloud Instrumentation	
Ceilometer (CEIL)	Vaisala Ceilometer (VCEIL)
Total Sky Imager (TSI)	Total Sky Imager (TSI)
Doppler Lidar (DL)	Doppler Lidar (DL)
Ka-Band Scanning ARM Cloud Radar (KASACR)	Ka-Band Scanning ARM Cloud Radar (KASACR)
Ka-Band ARM Zenith Radar (KAZR)	Ka-Band ARM Zenith Radar (KAZR)
W-Band Scanning ARM Cloud Radar (WSACR)	W-Band Scanning ARM Cloud Radar (WSACR)
Multipulse Lidar (MPL)	Micropulse Lidar (MPL)
Cloud Mask from Multipulse Lidar (MPLCMASK)	Radar Wind Profiler (RWP)
X-Band Scanning ARM Precipitation Radar (XSAPR)	C-Band ARM Precipitation Radar (CSAPR)
	Microwave Radiometer, 3-Channel (MWR3C)
	Raman Lidar (RL)
Radiometers	
Atmospheric Emitted Radiance Interferometer (AERI)	Atmospheric Emitted Radiance Interferometer (AERI)
Infrared Thermometer (IRT)	Infrared Thermometer (IRT)
Cimel Sunphotometer (CSPHOT)	Cimel Sunphotometer (CSPHOT)
Upwelling Radiation (GNDRAD)	Upwelling Radiation (GNDRAD)
G-band (183 GHz) Vapor Radiometer (GVR)	Groupings of broadband instruments such as pyranometers, pyrgeometers, and pyrheliometers.
G-band (183 GHz) Vapor Radiometric Profiler (GVRP)	
High Spectral Resolution Lidar (HSRL)	Multifilter Rotating Shadowband Radiometer (MFRSR)
Downwelling Radiation (SKYRAD)	Multifilter Radiometer (MFR)
Multifilter Radiometer (MFR)	Downwelling Radiation (SKYRAD)
Multifilter Rotating Shadowband Radiometer (MFRSR)	
Microwave Radiometer (MWR)	
Microwave Radiometer – High Frequency (MWRHF)	
Microwave Radiometer Profiler (MWRP)	
Normal Incidence Multifilter Radiometer (NIMFR)	
Surface Meteorology	
Meteorological Instrumentation (MET)	Meteorological Instrumentation (MET)
Facility-specific multi-level Meteorological Instrumentation (TWR)	Eddy Correlation Flux Measurement System (ECOR)
Ameriflux Measurement Component (AMC)	Ameriflux Measurement Component (AMC)
	Multi Angle Snow Camera (MASC)
AMF3 Phase III instruments *(to be added in the near future)* **Aerosol Observing System (AOS) to include**:	
• Ultra-High Sensitivity Aerosol Spectrometer	• Nephelometer, 3-wavelength
• Cloud Condensation Nuclei Counter (CCN)	• Two Condensation Particle Counters (CPC)
• Single Particle Soot Photometer (SP2)	• 7-Wavelength Aethelometer
• Scanning Mobility Particle Sizer (SMPS)	• Hygroscopic Tandem Differential Mobility Analyzer (HTDMA)
• Photo-Acoustic Soot Spectrometer (PASS)	• Particle Soot Absorption Photometer (PSAP)
• Humidigraph	

The Unmanned Aerial Systems (UAS) program supports aircraft measurements for priority scientific questions, including in-situ cloud properties, aerosol size, chemical composition, and remote sensing of various atmospheric parameters. Unmanned Aerial Systems (UAS) operations at Oliktok Point/AMF3 include TBS and UAVs. Some images from Oliktok Point/AMF3 field campaigns involving UASs are shown in Figure 3.

Tethered Balloon (TBS) Operation advantages include:

- Balloons allow for longer flight times.
- Can lift heaver instrumentation packages than typical UAVs.
- Slower rate of ascent and descent.
- Lower cost of operation compared to aircraft.
- Small crews are able to operate.

Unmanned Aircraft (UAV) Operation advantages include:

- Controllable flight to target specific areas of interest
- Can generally be operated by a small crew
- Small operational footprint for small UAV platforms
- Flights can extend over the oceanic regions offshore
- Potential for rapid deployment without significant set up/ tear down time
- Can ascend/descend quickly to sample targets of interest (e.g. clouds, aerosol layers)

Figure 3: UAS Operations from Oliktok Point/AMF3. (Clockwise from upper left): Tethered Helikite launch (Sep. 2014), Helikite with tethered sondes (Sep. 2014), ScanEagle (Arctic Shield, July 2015), DataHawk launch (COALA, Oct. 2014), DataHawk-2 (ERASMUS, Aug. 2015), Balloon Sonde launch (ERASMUS, Aug. 2015), BAT-3 and Aeryon Scout (NMSU UAV Tests, 2012).

Recent Collaborations

During 2014, there were 12 field campaigns based at ARM NSA sites (DOE, 2014). Field campaigns and collaborations that have been conducted at the ARM-NSA sites during 2015 include (DOE, 2015b):

1. Arctic Shield (July 2015) with US Coast Guard, Conoco-Phillips, Insitu/Boeing, NOAA, FAA, NSB and Era Helicopter; using ScanEagle platform.
2. Evaluation of Routine Atmospheric Sounding Measurements using Unmanned Systems (ERASMUS-I, Aug 2015) with CIRES/CU-Boulder; using DataHawk-2 platform.
3. TBS (Tethered Balloon System) (Sep and Oct 2015, AMF3) with CIRES/CU-Boulder using 35 m^3 helikite and Pilatus platform.
4. ARM Airborne Carbon Measurements on the North Slope of Alaska (ACME V) with Lawrence Berkeley National Lab, NASA, Pacific Northwest National Lab, Brookhaven National Lab, NOOA, Harvard University and University of Colorado; to observe atmospheric trace gases, aerosols, and cloud properties at the NSA.
5. Atqasuk GPS Base Station (ongoing through 2021) with UNAVCO; to provide GPS information to multiple users.
6. ARM Radiosondes for NPOESS/NPP Validation (ongoing) with NASA; for satellite data validation.
7. Support for Next-Generation Ecosystem Experiment (NGEE Arctic) (ongoing); to support data collection of Arctic ecosystem and climate feedback processes.
8. Barrow In-Situ Snow Sampling Study (ongoing through 2016) with Japan Agency for Marine Earth Science Technology (JAMSTEC); to analyze black carbon concentration and size distribution in snow.
9. Arctic Observing eXperiment (AOX, ongoing through 2016) with University of Washington; to provide data in support of modeling and information towards international Arctic/Antarctic programs.
10. EarthScope Seismic Station A21K-6 (ongoing through 2018) with IRIS; to operate a station among an array for seismic observations.
11. Arctic Methane, Carbon Aerosols, and Tracers Study (ongoing through 2016) with Sandia National Labs; to measure methane, black carbon, and source tracers in the atmosphere.
12. Micro-Climate Influences on Bird Arrival Behavior (2015) with Radford University; to study meteorological influences on behaviors of migrating birds.
13. Summertime Aerosol across North Slope of Alaska (ongoing through 2016) with University of Michigan; to study atmospheric chemistry and particulates to model local, regional and long range transport of NSA aerosols in the summer.

Tethered Balloon Operations

ARM is developing a tethered balloon system (TBS) capable of routine daily operations at Oliktok Point/AMF3. Operations will be conducted up to 7,000’ above ground level (AGL) within the R-2204 restricted area (Fig. 1, right), and the balloon will remain aloft for up to 18 hours per day. The TBS will operate within clouds to collect high vertical resolution atmospheric data. Increased vertical resolution of meteorological properties and cloud measurements will improve understanding of arctic cloud processes and complement the data concurrently obtained by existing AMF3 site instrumentation. Currently, the ARM TBS currently includes the following equipment:

- Two 35 m^3 helikites (14 kg (31 lbs) minimum lift at sea level (MLSL))
- One SkyDoc™ Aerostat (Model #26, 52.6 kg (116 lbs) MLSL)

- One SkyDoc™ Aerostat (Model #28, 54.9 kg (121 lbs) MLSL)
- Two 3050 meter (10 000 foot) tether capacity winches
- Two 460 meter (1500 foot) tether capacity winches

Current instrumentation used with the ARM TBS include:

- Sixteen tethersondes (measure pressure, relative humidity, temperature, wind speed, wind direction, altitude, latitude, longitude)
- Two upward-facing cameras to monitor the TBS in-flight
- Clinometer used to determine tether angle for redundant calculation of sensor altitude
- Wireless temperature and wetness/icing sensor
- Two supercooled liquid water content (SLWC) sensors

ARM has interest in procuring a distributed temperature sensing (DTS) fiber system. In practice, the DTS fiber would run along the balloon tether and sample temperature every 8 meters at a 30-second sampling rate with an accuracy of 0.06°C.

Science Objectives

The primary purpose of the ARM NSA sites is to provide comprehensive data sets to develop and test Global Climate Model algorithms to describe radiative transfer and cloud processes at high latitudes. Current objectives (DOE, 2015a) are to improve understanding of processes to describe:

- Radiative transfer in both clear and cloudy atmospheres, especially at low temperatures;
- Physical and optical behaviors of surface water (ice) and land, both bare and snow-covered, especially during transitions between winter and summer;
- Physical and optical behavior of ice and mixed phase clouds.

In September 2014, DOE held a workshop focused on scientific priorities for observational activities in the North Slope. Mixed-phase clouds, which contain both liquid droplets and ice particles, are the dominant cloud type over Polar Regions and have a large global coverage. The processes that cause mixed-phase clouds to form, grow, and dissipate are not well understood and are often poorly modeled. Predicting how atmospheric aerosols influence cloud formation and climate is a challenge that limits the accuracy of atmospheric models. This problem is especially true in the Arctic. Results (from the Indirect and Semi-Direct Aerosol Campaign (ISDAC) field study, 2008) also indicate that the number and composition of particles capable of forming clouds over Alaska can be influenced by episodic events such as biomass burning (for example, forest fires) that bring aerosols from the local vicinity and as far away as Siberia (DOE, 2014).

The DOE Atmospheric Systems Research (ASR) science team provides guidance on the types of measurements that most directly benefit the scientific community, involving four primary research themes: aerosol life cycle, cloud life cycle, cloud-aerosol interactions, and radiative processes. Current objectives revolve around these broad themes and five more detailed science subtopics, being:

1. Understanding clear-to-cloudy transitions, with a focus on single-layer low level clouds,
2. Characterization of North Slope aerosol properties and seasonal variability,
3. Understanding high-latitude aerosol-cloud interactions,
4. Characterization of North Slope cloud properties, and
5. Characterization of high-latitude precipitation processes, with emphasis on radar-centric evaluation of precipitation.

Understanding clear-to-cloudy transitions, with a focus on single-layer low level clouds: To understand the evolution of the lower troposphere during transitions from clear to cloudy conditions, frequent profiling of aerosol and thermodynamic properties of the lower atmosphere during the time period prior to stratiform cloud formation is a critical piece of information. There is also interest in measurement of the cloud-top region to assess properties relative to cloud lifetime. Another potentially important component to evaluate cloud lifecycle and lifetime is detailed measurement of the surface energy budget, with emphasis on turbulent surface fluxes, as well as onshore and offshore radiative and aerosol fluxes. Due to the coastal nature of the Oliktok Point and Barrow sites, having information on surface fluxes from the ocean/ice surface is important, particularly given the potential for the land surface to impact land-based measurements.

Characterization of North Slope aerosol properties and seasonal variability: Deployment of the Aerosol Observing System (AOS) in 2016 will enable data of seasonal variability in aerosol properties. However, because the Arctic atmosphere can be very stratified, translating surface aerosol properties to understand aerosol-cloud interactions and aerosol radiative impacts is unclear. Capabilities for routine profiling of aerosol properties would be beneficial, particularly during the late-winter and early spring Arctic Haze period, with intent to obtain representative sampling of all seasons and atmospheric conditions. Profiles should provide information on particle size distribution, absorption and scattering, and offer an opportunity to collect filter samples for evaluation of chemical composition and cloud nucleation properties. Information on cloud nucleation (cloud condensation nucleation (CCN) and ice nucleation (IN)) activity is a critical component of aerosol-cloud interaction studies.

Understanding high-latitude aerosol-cloud interactions: A major hurdle to improving our understanding of aerosol-cloud interactions is limited information on aerosol profiles. While surface-based measurements are available, frequent stratification of the Arctic atmosphere introduces uncertainty in use of this data. Therefore, profiles of basic information on aerosols (e.g. number, size) can shed substantial light on this issue. It is important to get information on cloud microphysical properties, with a focus on liquid water droplet properties. Measurements of droplet size distribution would provide key insight into how the cloud microphysics responds to changes in aerosol properties. Frequent sampling is required to build sufficient statistics; observing similar cases under both clean and polluted conditions. It is critically important to have frequent profiling of aerosol properties when single-layer liquid-containing stratiform clouds are present.

Characterization of North Slope cloud properties: This subject area can generally be handled using continuously operational remote (land-based) sensors. UAVs and TBS could provide in-situ measurements of cloud microphysical properties (liquid and ice particle size distributions, liquid and ice water path, ice crystal habit, etc.).

Characterization of high-latitude precipitation processes, with emphasis on radar-centric evaluation of precipitation: Efforts in this area are generally focused on development and evaluation of radar-centric precipitation rate and water content information, along with ice hydrometeor habit parameter development. Information to help tune and evaluate relevant radar retrievals will be of greatest help. This includes measurements of cloud microphysics, with a focus on ice habit and ice crystal size distributions; ideally measured in the cloud close to that sampled by the radar systems. Turbulence measurements throughout the cloud depth will improve turbulent mixing process assumptions.

In general, there are obstacles in using new sensors and platforms, such as those introduced for UASs. Characterization of sensor performance, error analysis, and evaluation of sensor operation under UAS deployment is critical to ensure that measurements are usable.

Future Prospects

The development of the Megasite concept for ARM NSA facilities provides opportunities for continued operations and research in Barrow, Oliktok Point and Atqasuk. Collaborations across ARM and with North Slope partners is expanding and bringing new skills and tools to support varied interests. With the extended deployment of AMF3, the establishment of controlled air spaces R-2204 and W-220, and having the northernmost surface road connection to the lower 48 States, Oliktok Point is well situated to serve expanded UAS and field operations. Promising discussions are in place to establish a long-term Science Camp at Oliktok Point in order to provide a stronger infrastructure, continue research and build on the observations from AMF3. With Federal Aviation Administration (FAA) approvals, UAVs can also operate out of Barrow or Atqasuk to provide coordinated operations along the North Slope. Testing of new sensors and approaches for data collection (e.g. drop sondes/gliders from tethered balloons) are but one area of interest for novel observations in the Arctic. The Unmanned Aerial Systems (UAS) program is expanding its capabilities and instrumentation to provide more frequent and sustained observations, with repeated flights to collect year-round data across a spectrum of atmospheric and surface conditions to compliment surface-based observations. The ARM NSA facilities provide a baseline of instruments and user facilities to support many users for research, search and rescue operations, wildlife management, earth studies and others. Ongoing and future field campaigns and collaborations are expected to provide important information to support the core mission of the DOE ARM NSA program, as well as partner programs.

Contacts

For further information on ARM NSA facilities and operations, please contact the persons below:

Mark Ivey
ARM NSA Facility Manager
mdivey@sandia.gov

Fred Helsel
AMF3 Site Manager
fmhelse@sandia.gov

Dan Lucero
Barrow Site Manager
dalucer@sandia.gov

References:

Department of Energy (DOE) ARM Program, 2014. ARM Climate Research Facility Annual Report-2014, DOE/SC-ARM-14-033. http://www.arm.gov/publications/annual-reports/docs/doe-sc-arm-14-033.pdf, (accessed October 14 2015).

Department of Energy (DOE) ARM Program, 2015a. ARM Climate Research NSA Science, http://www.arm.gov/sites/nsa/science, (accessed October 14 2015).

Department of Energy (DOE) ARM Program, 2015b. ARM Climate Research Field Campaigns, from field campaigns list at http://www.arm.gov/campaigns/table, (accessed and searched 14 October 2015).

The Need for Data and Technology Integration to Observe Tundra Wildfires at Multiple Scales

Arif Masrur and Andrey Petrov; Department of Geography, University of Northern Iowa, USA.

Email: masrura@uni.edu

Arctic systems are changing more rapidly than any other systems around the planet as a result of changing climate (IPCC 2007). As the Arctic plays major role in global climate feedback, any changes in the Arctic affects other parts of the world. The indispensability for observing changes in the Arctic brought people and institutions on a common platform for data acquisition and research. There are various networks and groups are already in place, formed by both Arctic and non-Arctic nations. Numerous studies have been carried out in different spatial and temporal scales on various dimensions of Arctic human and physical systems. Both field measurements and remotely sensed data have demonstrated their strength in identifying complex patterns of environmental changes. However, over the past decade there has been a growing need for circumpolar observation as a result of heterogeneous nature of challenges faced across the Arctic. Studies have shown that the nature and dynamics of wildfires in the North American Arctic and European Arctic tend to be different as a result of contrasting biophysical and bioclimatic factors (Rogers et al. 2015). To better understand the variations, patterns and processes of these phenomena, integrating regional dataset into a comprehensive global dataset has its merit in conducting circumpolar observation.

Existing satellite observing systems collect global datasets that is very useful as they provide necessary spectral bands to capture phenomena such as wildfires. A wide variety of global-scale satellite observations are currently available to monitor these events worldwide, however, only some of them have been engaged in conducting observation of polar environments. For instance, Fire Information for Resource Management System (FIRMS) delivers global fire locations (with fire intensity measures) in easy to use formats captured by MODerate Resolution Imaging Spectroradiometer on board NASA’s Earth Observing System (EOS) Terra (EOS AM) and Aqua (EOS PM) satellites. These are near real-time observations (available for the last 24 hours) of active fire hotspots that are useful for observing both global and regional changes in wildfire events. Temporal and spatial dimensions of these datasets facilitate tracking fire progression both spatially and temporally. That is, we can identify spatial and seasonal patterns of Arctic wildfires in relation to changing climatic parameters. We have been using these MODIS datasets to study the spatio-temporal dynamics of Arctic tundra wildfire on a circumpolar basis. However, the observations of these wildfires are only available since 2000 and onward. Another opportunity is to broadly and jointly use hyperspectral and moderate to high resolution imagery collected by early sensors and systems (e.g., Landsat, EO-1 Hyperion, SPOT) that also provide useful data to study wildfire events, but with limitations (Zhang et al. 2003). These observing systems were not developed in sole purpose to collect information from the Arctic. Moreover, there are disturbances involved (e.g., cloud cover) and also, they don’t provide finer-scale detail essential to make ground-to-satellite comparisons to study region-wide change (LaRue et al. 2013).

Although previous reports of the Arctic Observing Summit (AOS) have already discussed the need for ‘accurate and continuous’ data record, it is time to develop multiscale systems for simultaneous observations involving satellite, airborne and ground components. The wider use of low-altitude remote sensing instruments (UAVs) and methods could be effective in monitoring wildfire events in the Arctic at regional scales. However, not only high cost and technical difficulties are involved with these novel approaches, but also these applications are limited to small geographic area. In this perspective our suggestions are:

1) Create tundra wildfire knowledge hubs in key regions that will ultimately be integrated into circumpolar observation network;
2) Within these knowledge hubs, initiate simultaneous deployment of multiple sensors (both satellite, airborne/UAVs) and ground-based observation systems at regional scales to better understand the relationship between tundra's insitu bio-geo-physical characteristics (e.g. moisture stress, evapotranspiration, biomass, etc.) and remotely sensed data (hyperspectral, high-resolution, thermal, etc.);
3) Intensify data sharing and knowledge exchange that help various stakeholders in terms of cost-effectiveness, easy accessibility, reusability and efficiency;
4) Engage already existing global fire data more effectively in studying local/regional wildfire events in the circumpolar Arctic.

Literature Cited:

IPCC, 2007. Climate change 2007: synthesis report. Cambridge University Press. Available at http://www.ipcc.ch/publications_and_data/

LaRue, MA, Morin, P, and Pundsack J. 2013. Integrating high-resolution satellite imagery into the Arctic Observing Network through the Polar Geospatial Center.

Rogers BM, Soja AJ, Goulden ML, Randerson JT. 2015. Influence of tree species on continental differences in boreal fires and climate feedbacks. Nature Geoscience 8: 228–234.

Zhang YH, Wooster MJ, Tutubalina O, Perry GLW. 2003. Monthly burned area and forest fire carbon emission estimates for the Russian Federation from SPOT VGT, Remote Sens. Environ. 87, 1–15.

Permafrost Active Layer Seismic Interferometry Experiment (PALSIE) and Satellite Observations

Hunter Knox[1], Robert Abbott[1], Stephanie James[1,2], Rebekah Lee[1,3], and Chris Cole[4]

[1] Geophysics and Atmospheric Sciences, Sandia National Laboratories, Albuquerque, New Mexico, USA; [2] The University of Florida, Gainesville, FL, USA; [3] Boise State University, Boise, ID, USA; [4] Bureau of Land Management, Lakewood, CO, USA

Executive Summary: We present findings from a novel field experiment conducted at Poker Flat Research Range in Fairbanks, Alaska that was designed to monitor changes in active layer thickness in real time. Results are derived primarily from seismic data streaming from seven Nanometric Trillium Posthole seismometers directly buried in the uppermost section of the permafrost. The data were evaluated using two analysis methods: Horizontal to Vertical Spectral Ratio (HVSR) and ambient noise seismic interferometry. Results from the HVSR conclusively illustrated the method's effectiveness at determining the active layer's thickness with a single station. Investigations with the multi-station method (ambient noise seismic interferometry) are continuing and have not yet conclusively determined active layer thickness changes. Further work also continues with the Bureau of Land Management (BLM) to determine if the ground based measurements can constrain satellite imagery, which provides measurements on a much larger spatial scale.

1. Motivation

The potential feedback loop that may result from climate warming of high latitudes and the associated thawing of permafrost is of great concern to current and future climate change studies and projections. As climate warms, permafrost thaws and the active layer increases in thickness (Nelson et al., 2001). In the Northern Hemisphere, frozen relict soils contained in permafrost have high carbon content (Zimov et al., 2009). Therefore, the thawing of permafrost results in decay of previously frozen organic matter which then releases carbon to the atmosphere through bacterial respiration in the form of either carbon dioxide or methane, CO_2 or CH_4, respectively (Zimov et al., 2009; Schuur et al., 2008; Schuur et al., 2009). In addition, thawing of permafrost also causes subsidence and slope destabilization, both of which are critical to infrastructure, construction operations, and produce natural hazards (Nelson et al., 2001; Gruber et al., 2007). Monitoring changes in active layer thickness from year to year (building up to decadal trends) will provide invaluable information for many entities (i.e. DOD, DOE, DHS, BLM, USGS, etc). This project was designed to evaluate the hypothesis that changes in active layer thickness exhibit a noticeable difference in seismic velocities, that those changes could be monitored in real time, and this spatially limited information could be used to calibrate satellite imagery.

2. Site Description

The site location for this study was contained within a ~0.01 km^2 area at Poker Flat Research Range (PFRR), approximately 30 miles north of Fairbanks, Alaska. PFRR is a scientific research facility owned and operated by the Geophysical Institute of the University of Alaska. PFRR lies within the northern portion of what is known as the Fairbanks mining district of Alaska. This mining district was one of the most important gold producing areas in Alaska (Robinson et al., 1990). The site is situated along the northwest side of a slope that descends gradually to the Chatanika River, located approximately 1 km to the northwest from the site. Permafrost in the study region is discontinuous, meaning permafrost is typically no more than 50 m thick and talik zones are common (Schuur et al., 2008; Yershov, 1998). The study area is within the boreal forest ecoregion of interior Alaska as classified by Nowacki and others (2001). More specifically, PFRR lies in the Yukon-Tanana Uplands of the Intermontane Boreal ecoregion (Nowacki et al., 2001).

In the discontinuous permafrost zone that comprises our study site, permafrost generally occurs on north-facing slopes since they receive less direct radiation compared to south-facing slopes (Jorgenson et al., 2010). Also, the boreal forests of the study region can have an insulating effect on the soil, thereby contributing to factors controlling permafrost characteristics (Jorgenson et al., 2010). In turn, the presence and type of vegetation can be influenced by permafrost characteristics, and can sometimes be used as permafrost and active layer thickness/presence indicators. For example, the northwest portion of the site contains black spruce trees, which generally occur in poorly drained organic soils that are underlain by permafrost (Viereck et al., 1992). We would expect that active layer thicknesses and permafrost extents in the northwest portion are different than those in locations without black spruce trees on the study site.

3. Seismic Array

The primary data for this experiment was continuous seismic data collected with a small array deployed at PFRR. The array geometry is best described as two concentric circular arrays with 50 and 125m radii respectively. For this array, we chose to deploy seven Nanometrics Trillium Compact (TC) Posthole sensors. These state-of-the-art sensors were chosen because: 1) the instruments had self-noise levels below the USGS New Low-Noise Minimum Model (NLNM) at the frequencies of interests (> 1 Hz), 2) they are designed for direct burial, meaning they do not require a seismic vault or enclosure, and 3) the sensor has wide tilt tolerance (+/- 10 degrees from horizontal). Refraction Technologies (RefTek) Model 130 6-channel digitizers were chosen for the digital acquisition systems (DAS). The network was powered by extending 120V AC power to the center of the array from existing powered infrastructure. At the center of the array, we placed a Power-Over-Ethernet (PoE) hub, which distributed 40 Volts DC to the seven array elements. There the 40 Volts were reduced to 12 Volts by a DC-to-DC power converter. The array's close proximity to a building with power and Internet allowed us to install a physical Ethernet cable for communication. The RefTek 130s came with GPS clocks and antennas for timing. We installed the GPS antennas on T-posts high enough (about 1.5 meters) to be above the presumed snow depth.

4. HVSR Investigation

During the planning phases of this experiment, it was believed that computing the horizontal to vertical spectral ratios (HVSR) at each station would yield estimates of active layer thickness in real time. This was primarily due to the extremely high shear wave velocity contrast existing between the active layer and the permafrost. What was unknown at that time was the level of temporal resolution that could be achieved (i.e. the number of recorded days required to make a stable estimate).

We note that this method, while not obviously useful in the presence of presumably more temporally accurate methods (i.e. borehole thermometers), could supplement the existing information and provide estimates of active layer thickness for locations where it is either logistically difficult or economically unreasonable to drill a borehole, place a thaw tube, or visit the site regularly. Installing a seismic sensor in arctic conditions, as has been proven by the massive increase in the number of deployments in the last ten years, is less arduous and expensive than drilling a borehole. This method, like borehole measurements, is sensitive to only the area immediately surrounding the seismic sensor and therefore only provides spatially confined estimates. It is possible, as will be discussed later, that these measurements could be used to calibrate satellite imagery, which could provide estimates of active layer thickness and it's temporal response over much larger areas.

HVSRs are considered standard observations for shallow site classification (i.e. VS30, VS10), making it a widely applied methodology. The work using these observations spans a great number of applications from basement depth investigations to civil structure vulnerability assessments to depth determinations for remotely located shallow subsurface layers (e.g. Nakamura, 2009; Overduin et al., 2015). The computational routine used for our investigation relied on the GEOPSY software (www.geopsy.org) and used standard processing procedures as described in SESAME (2004). More information about the general technique can be found through those references. We will highlight study specific information below.

For this study, we report analysis from 3 stations installed by Sandia National Labs (SNL) in a valley with marshy summer conditions. These stations continuously recorded data at 125 samples per second. The data from 12AM to 4AM local time was selected for evaluation and a short-term average over long-term average (STA/LTA) algorithm was used to eliminate any high amplitude events. This time period was chosen because it was the least contaminated with spurious anthropogenic noise sources. During the initial evaluation of the HVSR observations, we found that stacking a week of observations provided a stable estimate (i.e. no significant deviations were seen in the spectral responses).

Results from this study, as illustrated in Figure 1, show seasonal peaks for stations CE1 and R1B, which were installed in a deforested region with relatively consistent active layer thicknesses (determined through tile probe measurements). Figure 1 also shows that station R2C, which is located in a black spruce forest, has no obvious seasonal trend. Specifically, the results show that during the winter months, when the ground is frozen to the surface, the stations exhibit flat spectral ratios above 6 Hz. As the ground thaws from the surface downward, there is increased variation at higher frequencies. We also observed a persistent peak at 2.5 Hz, which likely represents the depth to basement rock.

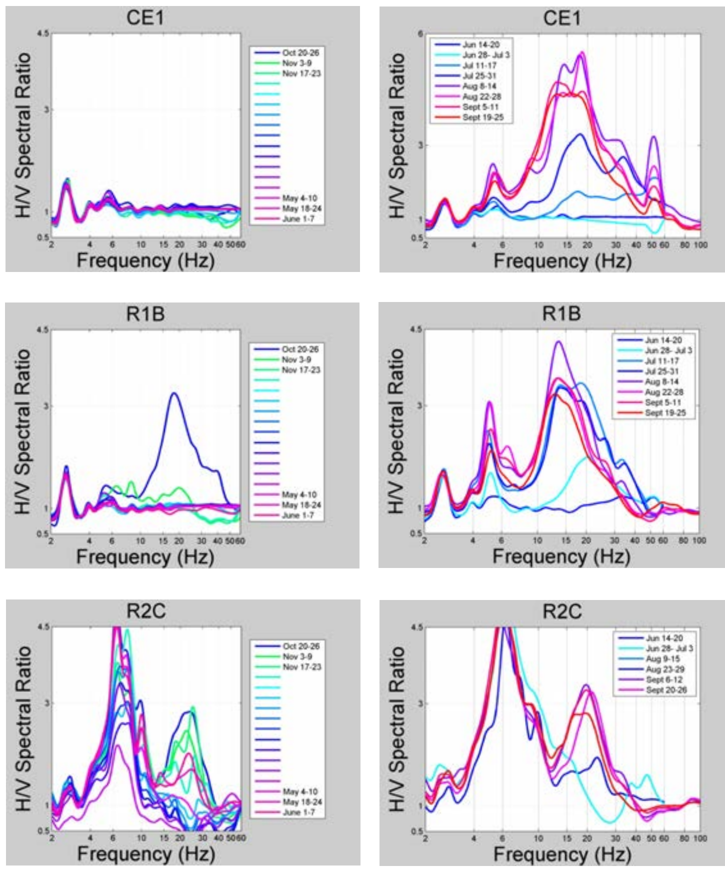

Figure 1: HVSR results for three stations at PFRR. The left column shows results for the winter months, while the right column illustrates the results for the summer months. Clear differences are seen between the stations that are likely tied to the terrain where the instruments were deployed.

We take this analysis one step further by using the quarter-wavelength approximation to estimate the active layer thickness. These thicknesses were computed for times when ground truth observations were taken. Using the quarter-wavelength approximation with h= 45 cm (thickness provided by June ground truth probing experiment), and Vs = 100 m/s (Holzer et. al, 2005; mud Vs) results in a peak at 55 Hz. This agrees nicely with the high frequency secondary peak. This peak migrates to 35 Hz, where a small shoulder is seen in HVSR, for 68 cm depth (October ground truth). These results support applicability of this method for determining seasonal changes. The quarter-wavelength approximation however cannot be used to explain the entire spectrum (i.e. peaks at ~15 Hz for summer CE1). We believe the larger amplitude peaks are caused by changes in Rayleigh-wave ellipticity. This effect has been shown to dominate in the presence of an extremely low-velocity surface layer (Flores et al., 2014).

5. Ambient Noise Seismic Interferometry

As research into ambient seismic noise characteristics expands, so too are the number of techniques for extracting valuable subsurface information from the noise wave field. In addition to the single-station HVSR method described earlier, records of ambient noise can also be used in multi-station methods. In particular, the most common technique for processing ambient seismic noise relies on the cross-correlation of records from a pair of stations. Under the assumption of a continuous and diffuse wave field generated by numerous natural and/or anthropogenic sources, the waves that are recorded at one station and propagate towards, and are recorded by, a second station can be cross-correlated to extract the impulse response (or Green's Function, GF) of the ground between the two stations (Shaprio & Campillo, 2004; Shapiro et al., 2005). With this technique, the first station becomes a virtual source for the seismic wave; therefore information about the actual source location is not needed. This gives ambient noise an advantage over traditional seismic methods involving ballistic waves generated from specific sources such as earthquakes or explosions (Shaprio & Campillo, 2004; Shapiro et al., 2005).

Having a 2-D array of stations and cross correlating all possible station pairs samples the subsurface repeatedly and provides a group velocity dataset than can then be used for tomographic inversion. In addition, the ambient noise wavefield is largely composed of surface seismic waves, i.e. Rayleigh and Love waves, which are dispersive, meaning different frequencies have different depth sensitivities. Differences in depth sensitivity provide vertical resolution, which is necessary for obtaining vertical velocity profiles. Using this conceptual set-up, numerous studies have successfully used ambient seismic noise for regional and continental scale 2-D and 3-D tomographic inversions for crustal structure (Shapiro et al., 2005; Sabra et al., 2005; Moschetti et al., 2007; Yang et al., 2007; Lin et al., 2008). However, recent studies have also been successful in exploiting later arrivals (coda) in ambient noise cross-correlations (CCs) for tracking temporal variations in subsurface velocity (Sens-Schonfelder & Wegler, 2006; Wegler & Sens-Schonfelder, 2007; Brenguier et al., 2008; Duputel et al., 2009; Mordet et al., 2010; Brenguier et al., 2011; Mainsant et al., 2012).

We used almost two years of nearly continuous ambient noise records from the 7 station PALSIE array to construct daily cross-correlation functions. The python package MSNoise was used to pre-process and calculate the correlations. We refer the reader to Bensen et al. 2007 and Lecocq et al. 2014 for more detailed information on the cross-correlation procedure. In addition to daily CCs, the

MSNoise package allowed for moving window stacks of pre-specified numbers of days to be computed. The correlations were then used for two separate multi-station ambient noise methods. The first method consisted of measuring the travel-time of the direct wave in order to construct group velocity dispersion curves to be inverted for 1-D shear velocity profiles. The main goal of this method was to assess if seasonal changes in the vertical velocity profiles resulting from winter versus summer dispersion curves could be retrieved. Detailed resolution of changes in active layer thickness was the main target, though shifts in permafrost depth range and thickness were also of interest. The second method employed was the Moving Window Cross-Spectral (MWCS) method using the python package MSNoise in order to construct semi-continuous time series depicting perturbations in subsurface velocity. The main goal of this method was to determine if ambient noise could be used for continuous monitoring of annual changes in active layer thickness as well as long-term degradation of permafrost resulting from climate change.

a. Group-Velocity Dispersion Curves & Vertical Velocity Profiles Results

The primary objective with respect to making measurements of group velocity was to determine if the GF resulting from correlations of ambient noise was seasonally affected. Changes from frozen ground in the winter to thawed ground in the summer results in a significant decrease in rigidity, which subsequently influences the velocity at which seismic waves propagate. Studies have documented reduced seismic velocities in thawed soil compared to frozen (Barnes, 1966; Zimmerman & King, 1986; Kneisel et al., 2008). Therefore, we hypothesized that the seasonal thawing of the active layer should be observable through a decrease in seismic velocity in summer compared to winter. The vertical transition between frozen and thawed soil at the permafrost table was expected to result in a velocity drop at a specific frequency range corresponding to waves most sensitive to the active layer. Thus, by utilizing the dispersive nature of surface waves it was hoped that the specific thickness of the active layer could be obtained.

We find that: 1) at low frequencies the summer and winter CCs are very similar and produce the same group velocity, 2) at a mid-high frequency range the summer signal-to-noise ratio is lower compared to the winter and the summer group velocity is significantly slower, and 3) at high frequencies the summer arrival is even slower still and the SNR remains lower compared to winter. The winter group velocity remains static between all three-frequency bands. We note here that frequency bandwidth had a large effect on the frequency-time plots and subsequent group velocity measurements. Another complication encountered was the prominence of multiple waveforms in the CCs. Stacking longer time periods helps to stabilize the CCs and typically results in the strong emergence of the direct arrival since that path is the shortest and most common compared to random scattered paths. However, even after stacking an average of 90 winter days and 85 summer days persistent arrivals continued to stack positively resulting in multiple prominent waveforms.

The network average winter and summer dispersion curves show similar velocities at frequencies below ~35 Hz (Figure 2). At higher frequencies a clear separation between the dispersion curves is observed, where the winter dispersion curve has consistently faster group velocities compared to summer.

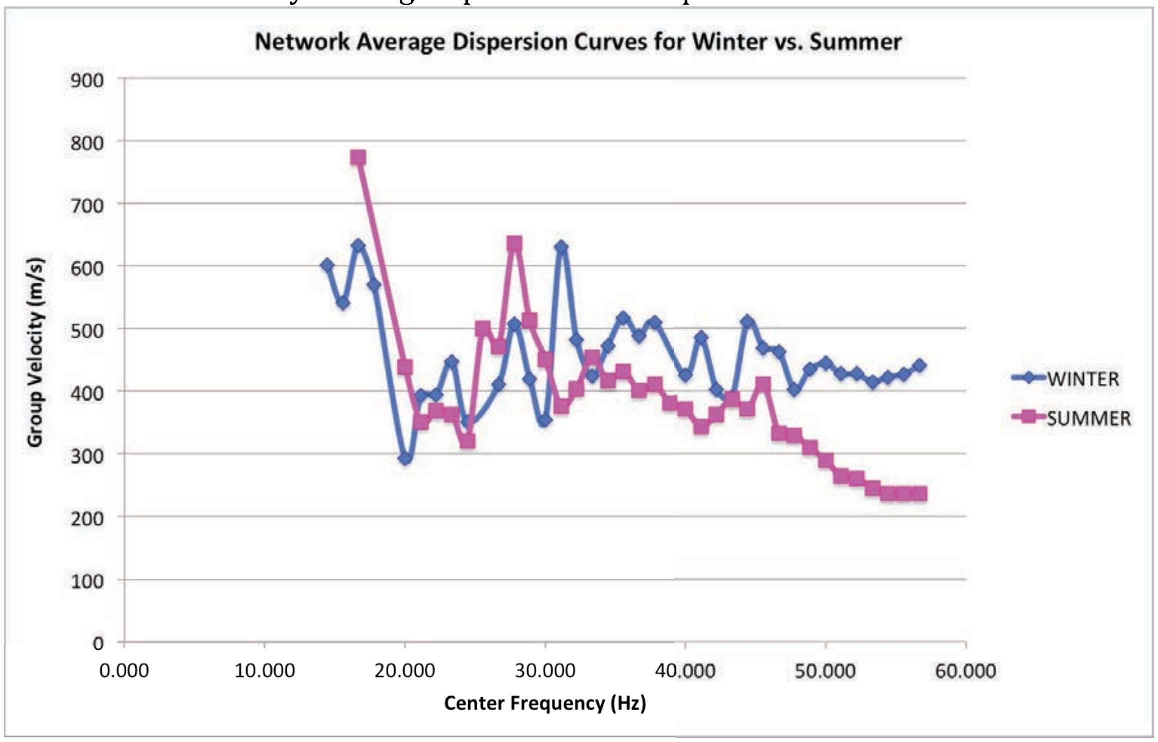

Figure 2: Network average dispersion curves for winter and summer. Note that the higher frequencies (> 35 Hz) show the most separation between winter and summer and are also better resolved compared to lower frequencies, which show more scattered.

The inversion results of the winter and summer dispersion curves show similar velocity structure below 6 meters depth (Figure 3). Above 6 m depth the winter velocity profile shows constant fast velocities within the range normal for frozen silt and organic rich soil (Barnes, 1966). The summer velocity profile shows slow velocities that gradual increase to 6 m depth. The depth sensitivity kernels produced by CPS show that the upper frequencies of the dataset have high sensitivity above ~5-6 m depth, however the sensitivities are the same in that depth range. This indicates that vertical resolution of the dataset is not sufficient to detect the specific thickness of the active layer. However, the slower velocities of the summer dispersion curve still produce a slow velocity zone at the shallowest depths. The maximum depth sensitivity of the dataset diminishes below ~24 meters depth.

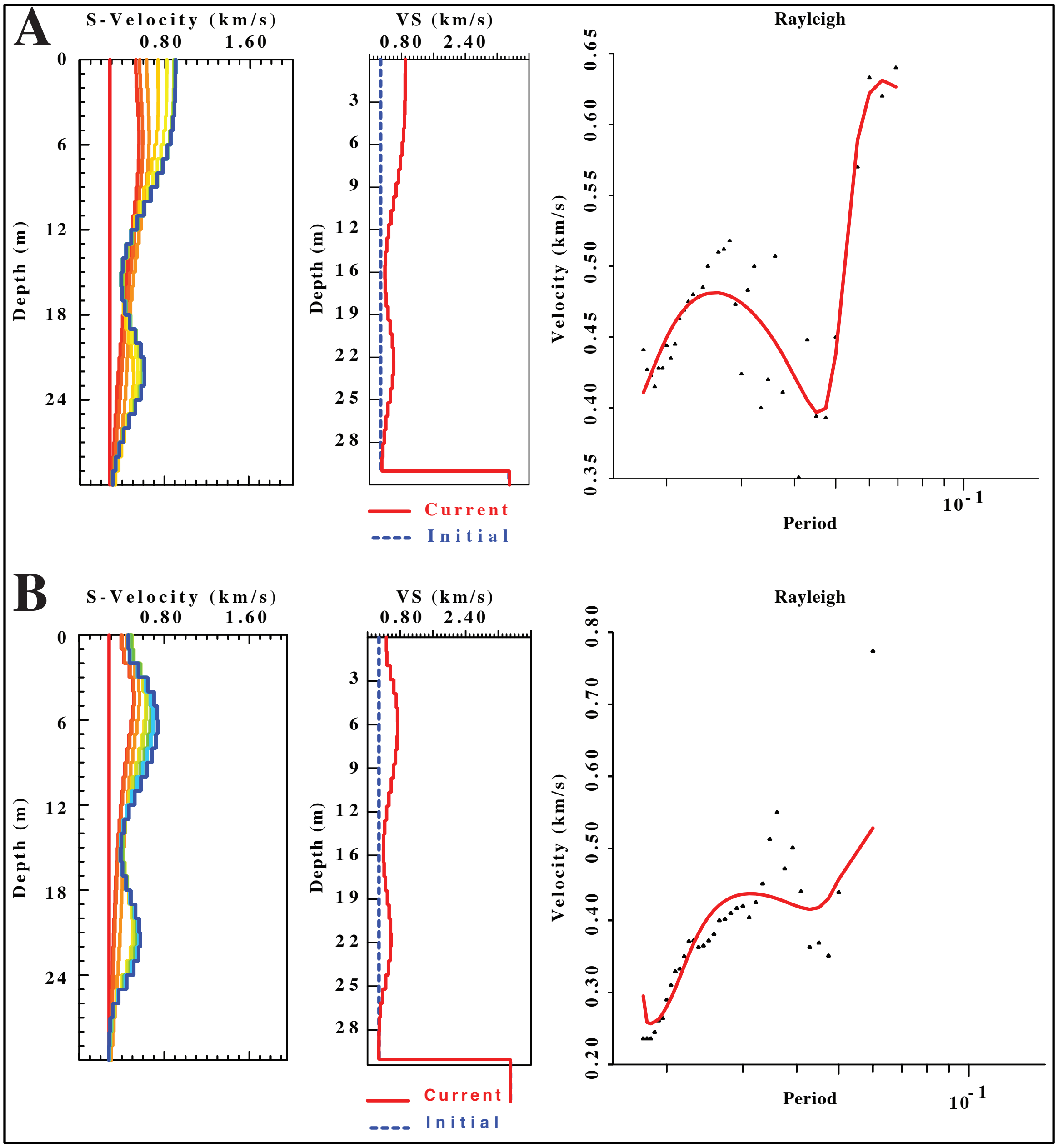

Figure 3: Results from iterative inversion using Computer Programs in Seismology (Herrmann & Ammon, 2002). Both winter (A) and summer (B) inversions start with the same constant velocity initial model (red in leftmost plots, blue in center plots). In subfigure (A), the final shear velocity profile (blue line in leftmost plot) resulting from the network average winter dispersion (center and rightmost plots) shows fast velocities from the surface down to 6 m depth followed by a gradual decrease to 15 m and subsequent increase to 22 m depth. In subfigure (B), the final shear velocity profile (blue line in leftmost plot) resulting from the network average summer dispersion (center and rightmost plots) shows slow velocities near the surface that increase down to 6 m depth followed by a decrease and increase matching that seen in the winter model. Both models navigate back toward the starting model below 24 meters depth, which is consistent with the maximum depth sensitivity.

b. Temporal Variation Results

The use of scattered seismic waves to monitor velocity changes of the subsurface was first proposed in the 1980s through analysis of seismic coda waves (Poupinet et al., 1984). This technique was later named Coda Wave Interferometry (CWI) (Snieder et al., 2002; Snieder, 2006). However, CWI relies on repetition of active sources, e.g. earthquakes, which can thereby result in discontinuous monitoring (Sens-Schonfelder & Wegler, 2006; Hadziioannou et al., 2009). Recent studies have sought the advantages of ambient seismic noise for use in monitoring applications, through a technique named Passive image interferometry (PII). PII combines the basic procedure of ambient noise cross-correlation with CWI to return measurements of temporal variations in seismic velocities of multiply scattered waves (Sens-Schonfelder & Wegler, 2006; Brenguier et al., 2008; Hadziioannou et al., 2009; Sens-Schonfelder & Wegler, 2011). PII has proven effective for a variety of applications such as detection of magma movement and changes in a volcanic edifice prior to eruption (Brenguier et al., 2008; Duputel et al., 2009; Mordet et al., 2010; Brenguier et al., 2011), co-seismic changes in fault-zone stress field (Wegler & Sens-Schonfelder, 2007), landslide prediction (Mainsant et al., 2012), and seasonal variations in hydrologic conditions (Sens-Schonfelder & Wegler, 2006).

Relative velocity changes were calculated for all station pairs for a variety of parameters and initial results from this analysis using the procedure defined by MSNoise are promising. A general trend is observed of more stable, lower amplitude $\delta v/v$ variations in winter followed by high amplitude variability in summer, regardless of the reference stack (January versus yearly average). An interesting outcome is the lack of a clear pattern of negative $\delta v/v$ values in summer and positive $\delta v/v$ values in winter. The summer months show both faster and slower velocities compared to the reference, which in the case of a January reference, is unexpected. There are a couple possible explanations for this: 1) the system could be more dynamic and complex than the simple transition from frozen to thawed ground as assumed, 2) that cycle skipping within the MSNoise analysis produces inaccurate measurements.

Overall, the findings from this portion of the PALSIE project indicate that monitoring velocity changes using ambient seismic noise is a promising new technique for permafrost studies. However, application of this method to the unique setting and characteristics of the Poker Flat dataset have led to complications not previously encountered in the seismic literature. Therefore customized procedures need to be developed.

6. Ground Truth Measurement Discussion

Here we summarize the three traditional (i.e. more common) datasets acquired throughout the course of the project. These datasets were acquired for two purposes: 1) To compare our results with more established methods; and 2) To use the results as constraints (i.e. ground truth) for the ambient noise methods. The CS survey adequately determined bulk velocities deeper than 3 meters. Coupled with the drilling reports, the method was also able to definitively measure the depth-to-bedrock. Unfortunately, the inability of the method to resolve shallow layers in this situation is a fatal weakness, as the active-layer was shallower than the uppermost resolved layer. Also, unknown factors (i.e. poor grout coupling, potential cross talk between the instrumentation) caused poor signal quality at certain depth intervals. ReMi measurements were extremely time consuming and difficult to acquire. Poor source and receiver coupling led to bandwidth-constrained dispersion curves. This in turn led to depth reconstructions, while consistent with tile probe measurements that poorly resolved deeper velocities and exhibited a general lack of uniqueness. Not surprisingly, as they are the "standard" method of active-layer thickness measurements, tile probing proved to be the most satisfactory method. Of course, it too suffers from the requirement of costly site visit, the resultant sparsity of the year-to-year datasets resulting, and the lack of any spatial and temporal resolution below the top of the permafrost. The latter could be important for understanding the deeper effects of changing active layer thickness in discontinuous permafrost regions.

All told, fusing the three methods yielded some improvement for determining the shallow velocity structure at the site. ReMi was unable to resolve deeper layers, while CS was unable to resolve shallower ones. ReMi suffered from non-uniqueness, but fixing active layer thickness with tile probe measurements and deeper velocity from CS resulted in an adequate model for our purposes.

7. Corresponding Satellite Observations

Permafrost changes and disturbances in Alaska pose potential human and environmental impacts, which must be tracked and characterized. Due to its geographic size, and varying climate, it is impractical to monitor all permafrost cover in Alaska using manual surveying methods. The ability to monitor permafrost cover trends using deployed, *in-situ* instruments (such as the array described here), and to integrate these measurements with multi-temporal remotely sensed imagery, would prove greatly beneficial to Alaska stakeholders (i.e. Bureau of Land Management).

Multi-scale, multi-temporal remotely sensed data were used for this study. Specifically, passive electro-optical (EO) imagery systems – those that require illumination from an external power source (i.e., the Sun) were used, including high-resolution commercial WorldView-2 and WorldView-3, and synoptic Landsat missions 5 and 8. A small number of WorldView-2 and WorldView-3 scenes were also available for this study. Additionally, landsat offered a multi-decadal historical archive, which was leveraged for this study. Lastly, multiple Synthetic Aperture Radar (SAR) systems were used, because of their ability to collect information regardless of solar illumination or weather condition. These SAR instruments chiefly included commercial Radarsat-2, and the European Space Agency's new Sentinel-1A instrument.

Image processing was needed for all but the Landsat data to allow quantitative geospatial analysis. This chiefly involved orthocorrection using digital elevation model (DEM) information to reduce geometric distortions, and increase geospatial positional accuracy. Additionally, all SAR data were calibrated to sigma-naught (Radar Cross Section) to allow quantitative pixel comparisons between sensor image dates. Finally, individual SAR scenes were "stacked" to form multi-band, time series image composites, based upon the sensor type (i.e., Radarsat-2, Sentinel-1A) and type of pass (ascending, descending). This was done to allow the images to be qualitatively assessed using traditional image interpretation techniques, and to allow image-to-image change detection. Finally, this also facilitated efficient extraction of pixel values for statistical trend analysis.

An object-oriented approach was used to develop a dataset, which could be used to identify spatio-temporal trends at PFRR. Using this approach, raster data pixels are grouped into meaningful image objects (vector polygons), based upon their spatial and spectral characteristics. An image segmentation (vector) dataset was produced from the high-resolution WorldView-3 imagery spanning the study area. Pixel value statistics were calculated for each Radarsat-2 and Sentinel-1A scene date, for each image object (including Poker Flat). The final vector polygon dataset contains the mean, median, minimum, and maximum pixel statistics extracted from each SAR image date.

The time series stacks for Radarsat-2 and Sentinel-1A were analyzed using several techniques. First, an interpretative (qualitative) analysis was performed, to identify and understand changes in landcover, or changes in landcover state, over the greater study area of interest. A time series analysis was then performed using the image segmentation dataset (populated with imagery pixel statistics). This allowed the identification of spatio-temporal trends over time and by sensor.

The use of Google Earth Engine (GEE) was also investigated and employed for this study. GEE is a cloud computing architecture, which allows the user to efficiently access, process, analyze, and develop products from large geospatial data archives. GEE proved greatly beneficial to this project, as it facilitated the analysis of spectral trends of land and water cover at PFRR over multiple decades by leveraging the entire U.S. Geological Survey (USGS) Landsat archive. This was accomplished without having to download the satellite data archive, nor devote local computational resources to process this massive dataset. Without the use of GEE, this analysis would not have been possible given the project's resources. As such, GEE clearly provides an emergent tool for the scientific community.

We developed custom GEE scripts, which calculated multiple spectral indices (shown to be useful for land and water cover studies) from available Landsat 5 and Landsat 8 data from 1984 to the present. The spectral indices included Normalized Difference Vegetation Index (NVDI), Normalized Difference Snow Index (NDSI, and Normalized Difference Water Index (NDWI). The script then extracted the median pixel values for each of the spectral indices (derived from each Landsat scene) spanning the study area, and produced a time series chart. This provided an unparalleled ability to characterize and visualize spatio-temporal spectral trends over the study site through multiple decades.

Preliminary results note a strong relationship between seasonal trends and remotely sensed observations. Our work suggests that spectral response in EO data, and in SAR backscatter measurements, differed with time of season. NDVI measurements at PFRR decreased strongly in winter, and increased strongly from spring to summer. This trend is likely due to phenology – that is, the increase in photosynthetic activity ("greenup") during the late spring and summer, and corresponding decrease in late fall to winter. Conversely, NDSI measurements at the site increased strongly in late fall to winter, and decreased significantly in summer. This is due to the presence of snow and/or ice cover. Time series analysis suggest SAR backscatter measurements followed a trend similar to that of the NDVI measurements - that is, an increase in backscatter during late spring to summer, followed by a decrease in winter. This trend was also confirmed by qualitative, interpretative analysis of the SAR multi-temporal imagery, and through change detection products derived from multiple SAR scene dates.

Conclusions

We presented here results from a two-year investigation that aimed to monitor active layer thickness in real time and link those observations (at least qualitatively) to satellite observations. Each part of this project yielded valuable information about the method's ability to determine active layer thickness, its spatial and temporal resolution, and the future challenges that must be overcome for these methods to be utilized. The HVSR method proved to be the most reliable and definitive in active layer thickness determinations, while the ambient noise seismic interferometry investigation showed complex results (previously undocumented) that will require future research. We also presented a way to combine ground truth data when each method is found to have weaknesses. Furthermore, we illustrated the difficulties in acquiring crosshole seismic and REMI data in these conditions. Finally, we present very preliminary results for the observations gained through analysis of satellite imagery. This work has only been conducted for a few short months, but shows great promise.

Path Forward

Future work on this project should continue on three fronts (HVSR, ambient noise seismic interferometry, and satellite observations), which we briefly highlight below. First, concerning the HVSR method and it's ability to determine active layer thickness, it will be paramount to invert the HVSR results with methodologies that can account for both Raleigh wave ellipticity and body wave resonances. The applicability of ambient noise seismic interferometery will require a more substantial amount of effort. Future work on this front includes conducting more rigorous group velocity measurements, evaluation of different stacking methodologies, evaluate spatial variation in the dispersion curves, generate sensitivity kernels for synthetic dispersion curves of frequencies higher than 60 Hz to identify the frequency range needed for resolving the active layer thickness, and running Markov Chain Monte Carlo (MCMC) inversions on representative group velocity dispersion curves (winter, winter-summer transition, summer, summer-winter transition) as alternate inversion method to the iterative method in CPS. Future work for the satellite comparison should include the acquisition and analysis of follow on Landsat 8, Sentinel-1A SAR, and ALOS PALSAR-2 remotely sensed imagery. The latter two instruments operate at different wavelengths (C- and L-Band, respectively), and offer different abilities to penetrate and resolve terrestrial cover information. While C Band SAR such as Sentinel-1A are very sensitive to surficial changes and disturbances, L-Band instruments such as ALOS are able to penetrate ground, and could be beneficial in characterizing permafrost, particularly when considering InSAR measurements. Also, the use of GEE should be further explored for this project as well. This could facilitate the integration of other geospatial datasets, including meteorological data and multi-scale remotely sensed observations into our methodological framework. GEE has begun ingesting Sentinel-1A SAR information into its burgeoning archive; this could streamline our efforts greatly. Finally, GEE offers numerous analytical capabilities and data classification algorithms not yet fully explored at present.

References

Abbott, R.E. (2013), Seismic Spatial Autocorrelation as a Technique to Track Changes in the Permafrost Active Layer, Abstract C43A-0661 presented at 2013 Fall Meeting, AGU, San Francisco, Calif., 10-14 Dec.

Brenguier, F., Shapiro, N.M., Campillo, M., Ferrazzini, V., Duputel, Z., Coutant, O., & Nercessian, A. 2008. Towards forecasting volcanic eruptions using seismic noise. Nature Geoscience, 1. 126-130.

Brenguier, F., Clarke, D., Aoki, Y., Shapiro, N.M., Campillo, M., & Ferrazzini, V. 2011. Monitoring volcanoes using seismic noise correlations. Comptes Rendus Geoscience, 343, 633-638.

Campillo, M., & Paul, A. 2003. Long-range correlations in the diffuse seismic coda. Science, 299, 547-549.

“Chatanika River Mine, Fairbanks District, Fairbanks North Star Borough, Alaska, USA,”. 8-7-15. http://www.mindat.org/loc-196874.html

Duputel, Z., Ferrazzini, V., Brenguier, F., Shapiro, N., Campillo, M., & Nercessian, A. 2009. Real time monitoring of relative velocity changes using ambient seismic noise at the Piton de la Fournaise volcano (La Reunion) from January 2006 to June 2007. Journal of Volcanology and Geothermal Research, 184, 164-173.

Flores, J.P., Garcia-Jerez, A., Luzon, F., Perton, M., F. Sanchez-Sesma. *Inversion of H/V ratio in layered systems*. AGU Fall meeting 2014.

Gruber, S., & Haeberli, W. 2007. Permafrost in steep bedrock slopes and its temperature-related destabilization following climate change. Journal of Geophysical Research, 112, F02S18.

Hadziioannou, C., Larose, E., Coutant, O., Roux, P., & Campillo, M. 2009. Stability of monitoring weak changes in multiply scattering media with ambient noise correlation: laboratory experiments. Journal of Acoustical Society of America, 125, 3688-3695.

Jorgenson, M. T., Shur, Y. L., & Pullman, E. R. (2006). Abrupt increase in permafrost degradation in Arctic Alaska. Geophysical Research Letters, 33(2).

Jorgenson, T. Yoshikawa, K., Kanevskiy, M., Shur, Y., Romanovsky, V., Marchenko S., Grosse, G., Brown, J., & Jones, B. 2008. Permafrost Characteristics of Alaska. Ninth International Conference On Permafrost (map).

Lee, R.F., R. E. Abbott, H. A. Knox, and A. Pancha (2014), Seasonal Changes in H/V Spectral Ratio at High Latitude Seismic Stations, Abstract S41A-4438 presented at 2014 Fall Meeting, AGU, San Francisco, Calif., 15-19 Dec.

Lin, F.C., Moschetti, M.P., & Ritzwoller, M.H. 2008. Surface wave tomography of the western United States from ambient seismic noise: Rayleigh and Love wave phase velocity maps. Geophysical Journal International, 173, 281-298.

Lobkis, O.I., & R.L Weaver. 2001. On the emergence of the Green's Function in the correlations of a diffuse field." Journal of Acoustical Society of America ,110.
Sens-Schonfelder, C., & Wegler, U. 2006. Passive image interferometry and seasonal variations of seismic velocities at Merapi Volcano, Indonesia. Geophysical Research Letters, 33, L21302.

Louie, J. N., 2001, Faster, better: Shear-wave velocity to 100 meters depth from refraction mi-crotremor arrays: Bulletin of the Seismological Society of America, 91, no. 2, 347–364.

Mainsant, G., Larose, E., Bronnimann, C., Jongmans, D., Michoud, C., & Jaboyedoff, M. 2012. Ambient seismic noise monitoring of a clay landslide: Toward failure prediction. Journal of Geophysical Research, 117, F01030.

McMechan, G.A., and Yedlin, M.J., 1981, Analysis of dispersive waves by wavefield transfor-mation: Geophysics, v. 46, p. 869-874.

Mordret, A., Jolly, A.D., Duputel, Z., & Fournier, N. 2010. Monitoring of phreatic eruptions using interferometry on retrieved cross-correlation function from ambient seismic noise: Results from Mt. Ruapehu, New Zealand. Journal of Volcanology and Geothermal Research, 191, 46-59.

Mortensen, J.K. 1992. Pre-Mid-Mesozoic Tectonic Evolution of the Yukon-Tanana Terrane, Yukon and Alaska. Tectonics, 11. 836-853.

Nelson, F., Brown, J., Lewkowicz, T., & Taylor, A. (1996). Active layer protocol.ITEX manual, 14-16.

Nelson, F.E., Anisimov, O.A., & Shiklomanov, N.I. 2001. Subsidence risk from thawing permafrost. Nature, 410, 889.

Newberry, R.J., Bundtzen, T.K., Clautice, K.H., Combellick, R.A., Douglas, T., Laird, G.M., Liss, S.A., Pinney, D.S., Reifenstahl, R.R., & Solie, D.N. 1996. Preliminary Geologic Map of the Fairbanks Mining District, Alaska. State of Alaska Department of Natural Resources, Division of Geological & Geophysical Surveys, Public-Data File 96-16.

Nowacki, G., Spencer, P., Brock, T., Fleming, M., & Jorgenson, T. 2001. Ecoregions of Alaska and Neighboring Territory. U.S. Geological Survey Open-File Report 02-297 (map).

Robinson, M.S., Smith, T.E., & Metz, P.A. 1990. Bedrock Geology of the Fairbanks Mining District. Alaska Division of Geological & Geophysical Surveys Professional Report 106, 2 sheets, scale 1:63,360. doi:10.14509/2287

Sabra, K.G., Gerstoft, P., Roux, P., Kuperman, W.A., & Fehler, M.C., 2005. Surface wave tomography from microseisms in Southern California. Geophysical Research Letters, 32, L14311.

Sens-Schonfelder, C., & Wegler, U. 2011. Passive image interferometry for monitoring crustal changes with ambient seismic noise. Comptes Rendus Geoscience, 343, 639-651.

Shapiro, N.M., & Campillo, M. 2004. Emergence of broadband Rayleigh waves from correlations of the ambient seismic noise. Geophysical Research Letters, 31, L07614.

Shapiro, N.M., Campillo, M., Stehly, L., & Ritzwoller, M.H. 2005. High-resolution surface-wave tomography from ambient seismic noise. Science, 307, 1615-1618.

Schuur, E.A.G., Bockheim, J., Canadell, J.G., Euskirchen, E., Field, C.B., Goryachkin, S.B., Hagemann, S., Kuhry, P., Lafleur, P.M., Lee, H., Mazhitova, G., Nelson, F.E., Rinke, A., Romanovsky, V.E., Shiklomanov, N.,Tarnocai, C., Venevsky, S., Vogel, J.G., & Zimov, S.A. 2008. Vulnerability of permafrost carbon to climate change: Implications for the global carbon cycle. Bioscience, 58, 701-714.

Schuur, E.A.G., Vogel, J.G., Crummer, K.G., Lee, H., Sickman, J.O., & Osterkamp, T.E. 2009. The effect of permafrost thaw on old carbon release and net carbon exchange from tundra. Nature, 459, 556-559.

Snieder, R. , Gret, A., Douma, H., & Scales, J. 2002. Coda Wave Interferometry for estimating nonlinear behavior in seismic velocity. Science, 295, 2253-2255.

Snieder, R. 2006. The theory of Coda Wave Interferometry. Pure and Applied Geophysics. 163. 455-473.

Viereck, L.A., Dyrness, C.T., Batten, A.R., Wenzlick, K.J. 1992. The Alaska Vegetation Classification. United States Department of Agriculture, Forest Service, General Technical Report PNW-GTR-286.

Weaver, R.L., & Lobkis, O.I. 2001. Ultrasonics without a source: Thermal fluctuation correlations at MHz frequencies. Physical Review Letters, 87, 134301.

Wilson, F.H., Dover, J.H., Bradley, D.C., Weber, F.R., Bundtzen, T.K., & Haeussler, P.J. 1998. Geologic Map of Central (Interior) Alaska. U.S. Geological Survey Open-File Report OF 98-133

Yang, Y., Ritzwoller, M.H., Levshin, A.L., & Shapiro, N.M. 2007. Ambient noise Rayleigh wave tomography across Europe. Geophysical Journal International, 168, 259-274.

Yershov, E. 1998. General Geocryology. Cambridge (United Kingdom): Cambridge University Press.

Zimmerman, R.W., & King, M.S. 1986. The effect of the extent of freezing on seismic velocities in unconsolidated permafrost. Geophysics, 51, 1285-1290.

Zimov, S.A., Schuur, E.A.G., Chapin III, F.S. 2009. Permafrost and the global carbon budget. Science, 312, 1612-1613.

2015 Arctic Observing Summit
Theme: Technology and innovation for sustained Arctic observations

Microbuoys for low-cost observation of the upper Arctic Ocean

Authors:
Alice Bradley, Scott Palo, Gabe LoDolce, Doug Weibel, Dale Lawrence, James Maslanik
Aerospace Engineering Sciences, University of Colorado Boulder
Chris Zappa
Lamont-Doherty Earth Observatory

Abstract

Small, instrumented buoys known as microbuoys provide a low cost means of acquiring measurements from the upper Arctic Ocean. They carry a small sensing suite (including GPS), a low-power microcontroller, a limited battery package, and a satellite modem or other radio for data retrieval. The platform is effectively agnostic of sensor type, though certainly limited by size and mass. For relatively low duty cycle sensing, battery capacity can last on the order of one month in a buoy of less than one liter in volume. The microbuoy concept was demonstrated in the Arctic during the 2013 MIZOPEX campaign, a NASA-run program that, among other things, deployed eight Air Deployed Microbuoys from unmanned aircraft in the Beaufort Marginal Ice Zone. The ADMB system is described, along with the general microbuoy concept and a few other examples of microbuoys. The Drone Deployed Micro-Drifter is a similar system that also integrates the functionality of a dropsonde, collecting atmospheric profile measurements as it falls into the ocean. The potential role of microbuoys in the Arctic observing system is described, with some comments on the best uses for these systems.

Microbuoy Concept

A microbuoy is fundamentally just that – a very small buoy. It caries a small set of sensors, operates largely autonomously for a period of weeks to a month, with sporadic data uploads either via satellite communication links or more local radio. While it lacks the extensive sensor suites of larger more complex buoys, or the extended lifetime from carrying solar panels or other power generation capabilities, the microbuoy is inexpensive, easy to deploy, deployable in conditions not suitable for larger buoys, such as within pack ice and near shore, and has a minimal impact on the surrounding oceanographic conditions.

Microbuoys are designed to be disposable. The intention is to be able to deploy several at once in order to get information on spatial patterns, or to toss one in the ocean to get measurements at a specific geographic point. Therefore they must be inexpensive (though what that means varies with the target measurements) to build, transport, and deploy. Materials used should be safe to leave in the ocean, and at small enough quantities that they do not pose a risk to the local ecosystem.

Because of the small size, microbouys can be deployed from a number of platforms. They should be built with sufficient ruggedness to survive a drop into the ocean from an aircraft. If they are intended to be dropped on ice, extra padding or a parachute or streamer may be necessary. With that requirement satisfied, the buoys are effectively agnostic to deployment mechanism and can take advantage of regular traffic in the region. Possible deployment vessels include ship traffic (research vessels, coast guard/military vessels, or private ships), aircraft (private, scientific, or domain awareness flights), or by hand from either shore or drifting stations. With sufficiently light microbuoys, even small, unmanned aircraft systems (UAS) can drop buoys at target locations.

The small profile of a buoy allows it to have a minimal impact on the surrounding ocean. A CTD profile cannot measure the top few meters of the surface mixed layer due to mixing from the impact with the surface. Large buoys similarly affect the water in immediate contact with the main part of the float, through solar and dissipative heating of the body. At the other end of the spectrum, an infinitesimally small buoy would have zero influence on the surrounding water, so it follows that a smaller buoy will have less impact than a larger one. Combined with the low power consumption of a tiny system, microbuoys provide a means to get sensors into the uppermost parts of the ocean without significantly impacting the surrounding seawater.

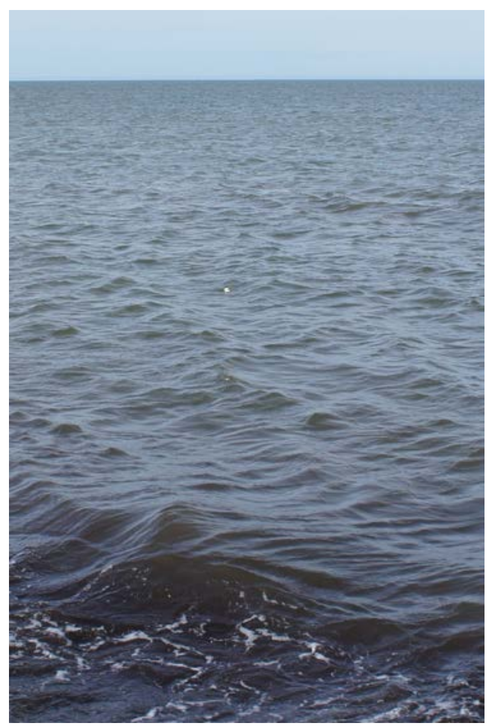

Figure 1: Air-deployed Microbuoy (white dot, center of image) drifting just offshore in the Arctic Ocean.

One example of microbuoys used for Arctic research is the Air-Deployed Microbuoy (ADMB), developed at the University of Colorado Boulder for the Marginal Ice Zone Observations and Processes Experiment (MIZOPEX) campaign; this system is described in more detail in the following section. The Drone Deployed Micro-Drifter is a similar instrument , with increased sensing capability both in the ocean (conductivity sensors on the sensor string) and atmospheric profiling sensors (temperature, pressure, relative humidity) for the descent.

Prior to recent development in Arctic-targeted and UAS-based systems, the microbuoy concept has been around since at least the early 2000s. The DMB evolved from an earlier miniaturized dropsonde successfully deployed from Aerosonde UAS in Antarctica in 2010 (Cassano et al., 2010). Micro Wave Sentry buoys, weighing in at just over 500g, are a downscaled version of larger Wave Sentry buoys built for event-duration monitoring of local sea state. The micro version of these lacks the GPS, but otherwise behaves like its larger counterpart for a short lifetime (days). Further description of the systems are in (McGehee and Earle 2002).

MIZOPEX campaign example

In July-August of 2013, NASA's Marginal Ice Zone Processes Experiment (MIZOPEX) demonstrated the use of microbuoys in the Arctic. MIZOPEX aimed to study ice-ocean interactions in the Marginal Ice Zone north of Oliktok Point, Alaska. Several UAS systems were flown during the campaign, carrying various types of sensors. The primary science goals of the project were related to understanding marginal ice zone dynamics and air-ice-ocean interactions in the region.

The Air-Deployed Micro Buoy (ADMB) was developed for the campaign and deployed to measure near-surface temperature gradients and ocean surface currents. Detail on the ADMB system and science results from the 2013 campaign are found in (Bradley et al. 2015).

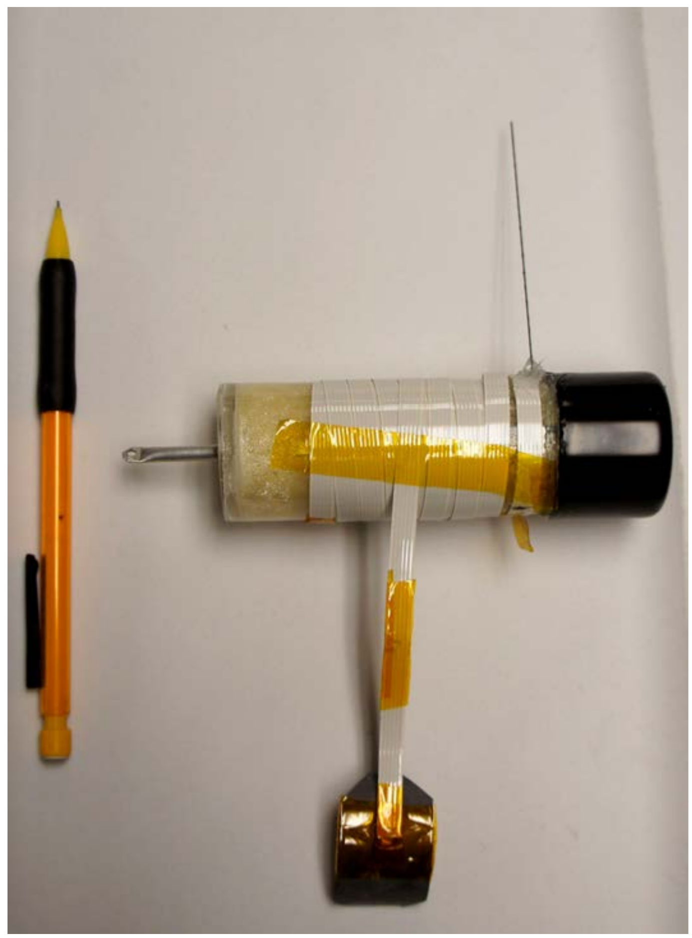

Figure 2: ADMB with thermistor string partially rolled up for launch. The whip antenna is for the data retrieval radio, and the sting at the left end is for attachment to the launch system.

The ADMB, pictured in **Figure 2**, is a microbuoy that measures near-surface temperatures and location. The buoy consists of a main body containing the electronics, battery, and communication systems imbedded in foam to protect on impact and enclosed in a waterproof case. From this, a string with the temperature sensors extends down two meters into the upper ocean, with thermistors at 3cm, 1m, and 2m below the ocean surface. The thermistors on the string are sampled by an analog-digital converter, the location and time stamp are determined by the GPS, and a 900 MHz radio is used to uplink data. Additional specifications are provided in **Table 1**. The ADMB was developed as a research effort, and so manufacturing cost is hard to estimate. Parts involved totaled to approximately $200, though without the benefit of scaled production.

Buoy size	11 cm long 3.2 cm diameter 87 cm^3 volume
Buoy mass	~90g
Radio	900 MHz Xbee radio
Radio range	3-5 km (weather dependent)
Battery	1000 mAh >10 days operation
Thermistor locations	3cm, 1m, 2m below surface
Thermistor accuracy	0.1 °C

Table 1: ADMB specifications for the model developed for MIZOPEX.

The real innovation of the ADMB system during MIZOPEX was in the deployment and operational use, sketched out in Figure 3. A set of AMDB are loaded into the UAS, which is programmed with drop points. The aircraft takes off and flies out to the area of interest. Once within a pre-set tolerance of the intended drop location, the communication board (doubling as the launch system) pulls a pin, releasing springs that eject the ADMB from the aircraft. The string and antenna are bound in water-soluble tape in order to keep from interfering with the aircraft propeller on ejection. Once it hits the water, the ADMB unravels, with the thermistor string extending down and the communication antenna popping up. The position of the battery inside the cylindrical buoy body keeps it upright, and the weighted thermistor string dampens rocking due to wave action.

In the water, the ADMB samples the thermistors once every six minutes and the GPS once per hour. This data is logged on the onboard SD card, which can store an entire battery lifetime's worth of measurements. When not in use, sensor sampling and GPS components are powered down to conserve power and minimize heating of the buoy. Meanwhile, the radio is cycling on a low duty cycle and listening for the high-repeat-frequency ping from the UAS-based communication board. When that signal is detected, the buoy transmits all data logged since the last upload. This does require that the aircraft come within radio range of the AMDB (approximately 5 km, weather dependent). For the MIZOPEX campaign, this was a sensible approach, as aircraft carrying down-looking sensors were flying lawn-mower patterns over the area making surface measurements.

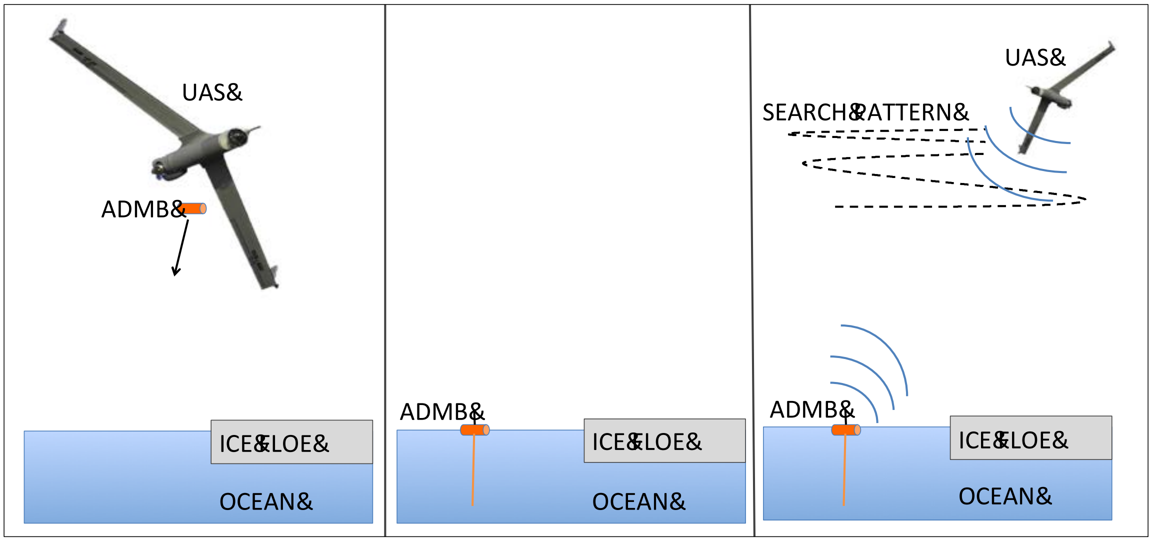

Figure 3: Concept of operations for the ADMB during the MIZOPEX campaign. A UAS drops the buoy into open water, leaves the area, and then at some later time returns with a communication board which pings the microbuoy and retrieves logged data. The communication board can be carried along with other science instruments for efficient use of flight time. Figure reproduced from Bradley et al. (2015).

ADMB deployments during MIZOPEX were limited due to severe weather and aircraft issues, but several days of data were collected at the end of the campaign in early August. Temperature measurements show significant near-surface temperature gradients on days with lower winds (and correspondingly minimal mixing). Areas with approximately zero ice concentration showed strong positive temperature gradients, with solar absorption at the surface creating a very warm (4-6 °C), positively buoyant layer that extended less than two meters into the water column. Areas with some ice cover (5-15%) often exhibited strongly negative temperature gradients, with cold, fresh water from melting floes pooling at the surface (Bradley, Palo, Maslanik, et al. 2014; Bradley et al. 2015). ADMB drift tracks showed the inertial oscillations resulting from Ekman drift in a rapidly changing wind field that are rarely detectable by larger buoys with longer sensor strings (Bradley, Palo, Zappa, et al. 2014).

ADMBs deployed during the MIZOPEX campaign proved to be resilient and reliable. Prior to aircraft deployments, several microbuoys were dropped into the ocean from shore and spent 7-10 days being bashed against a sandbag sea wall through a significant storm. One microbuoy was buried in sand during this storm, but was still able to make radio contact with a communication board on a UAS flying overhead, which led to its eventual retrieval.

DDμD System Example

The Drone Deployed Micro-Drifter (DDμD) payload consists of a Receiver module, a Launcher module, and the individual Micro-Drifters (or Drifters), supported by a central payload computer and INS acquisition system. The Drifters are small (<1lb), disposable electronics with their own integrated GPS receivers and IC sensors which measure air pressure, air temperature, relative humidity, water conductivity, and water temperature.

The Receiver module serves as a data relay between the payload computer and Drifter, and it monitors and maintains the battery charge on a Drifter while loaded into the Launcher. Any time a Drifter is in range of the Receiver, Drifter data are relayed through the Receiver to be recorded on the payload computer. The Receiver also interfaces through the payload computer and UAV autopilot coms to the UAV ground station. This interface allows for an operator to send remote, in-flight launch commands and also allows for data collection and remote recording to the UAV ground station while the Receiver is in range of a Drifter.

The Drifter is programmed to behave in two operational modes: atmospheric profiler and conductivity/temperature drifting buoy. The Drifter turns on in the profiler operational mode at the moment of launch. As it is falls through the atmosphere, the air pressure, air temperature, and relative humidity data are transmitted to the Receiver and recorded at 10 Hz on the main payload computer. Once the Drifter contacts the water surface, onboard accelerometers see the deceleration and switch the Drifter into the drifting buoy operational mode. Water-soluble material dissolves and releases a chain of conductivity and temperature sensors at depths of 0.1m, 0.4m, and 1.0m. The drifting buoy operational mode is set to record bursts of 10 samples every 15 minutes to onboard, non-volatile Drifter memory. This sampling scheme gives approximately 1 week of battery life for a particular Drifter.

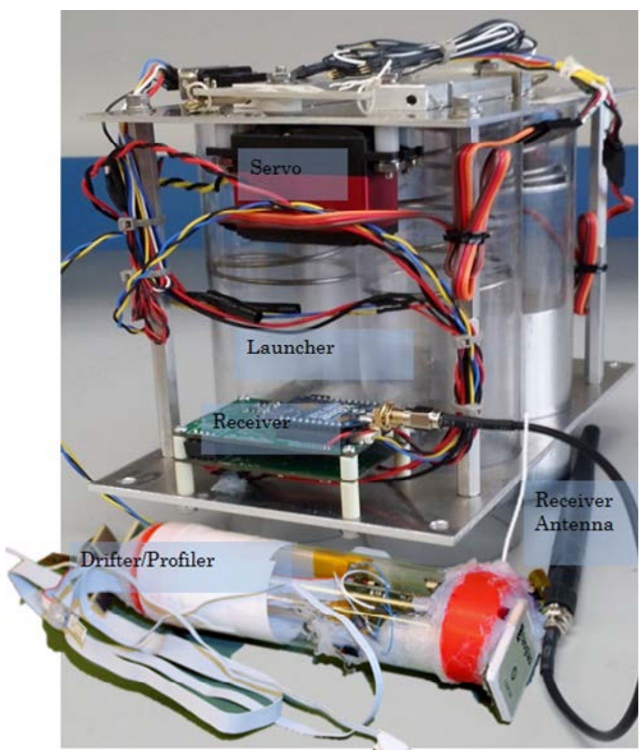

Figure 4: Drone Deployed Micro-Drifter (bottom) and support hardware.

On successive DDμD payload deployments, once the Receiver is back within the effective transmission range, the Drifter sends its onboard data to the Receiver, and the drifting buoy data recorded since launch is recorded to the payload computer. Successive DDμD payload deployments and data collections can continue for as long as a Drifter battery can provide power. **Error! Reference source not found. 4** shows one of the Drifters with the Receiver and tube Launcher integrated together to fly on the Manta UAV.

Future Development

The next step in microbuoy development is to remove the dependence on short-range radio retrieval for data collection. Through satellite communication links, microbuoys become fully autonomous and can operate at their full capacity regardless of deployment method. The ADMB is currently undergoing a redesign to upgrade to an Iridium short burst data link for data retrieval. While this increases the component cost of the microbuoy, it eliminates the need for aircraft time to re-visit the buoy's location to retrieve the data. The buoy can be programmed to upload data at a fixed interval (e.g., twice daily) so that up-to-date observations are available online in a timely manner but minimal battery capacity is used on powering up the radio frequently. Despite the fact that the satellite modem consumes more power than the short-range radio, saving on the duty cycle saves power overall.

Using a satellite link for data retrieval opens up the use scenarios as well. With the small size, buoys can be dropped from a variety of manned aircraft (i.e., small fixed-wing airplanes through an open window or out of the back of a Coast Guard C-130). UAS present additional challenges with changing aircraft center-of-gravity associated with dropping things, but as MIZOPEX demonstrated, deployment from small (under 50lb.) UAS is possible. Microbuoys are small enough to hold by hand, so they can be easily dropped over the edge of a ship, drill platform, or drifting station, and their small size and weight allows deployment of numerous buoys if desired.

The microbuoy platform is agnostic of sensor type, so long as the sensors are lightweight, small, and draw relatively little power. The ADMB carried a string of thermistors, but these could be supplemented by salinity sensors (Broadbent, Ivanov, and Fries 2007) or accelerometers for sea state observations. Additional sensors are possible so long as the form factor is sufficiently small and rugged for integration: sensors placed in contact with sea water should obviously be waterproofed in a manner such that saltwater will not damage the system for the lifetime of the battery. Some sensors (e.g., accelerometer) can be housed inside the buoy body, which provides a protective cover.

With the increased size in buoy from the AMDB to a microbuoy that can accommodate a satellite transceiver, there is capacity for increased battery mass while maintaining buoyancy. The exact battery capacity depends on both the mass (which is determined by the packaging) and the battery chemistry, but a 30-day lifetime is very reasonable. Along with the increased battery life, there is potential to change the form-factor in order to fit existing deployment methods for other systems such as dropsonde or expendable batho-thermograph (XBT) deployment equipment.

Role of microbuoys in AOS

The microbuoy platform provides and inexpensive and easy-to-deploy system for getting measurements in otherwise hard-to-monitor locations. Upper ocean processes in the Arctic are increasing in importance as the ice-free season extends, and microbuoys may prove to be important supplements for larger buoy systems in the region.

Larger, more robust systems are still prone to environmental stresses and do not tend to last for more than a season. The microbouy concept takes the three to five month lifespan of one larger system and replaces it with five microbuoy systems over the period of interest. It does depend on periodic access to the region of interest, but this can be accomplished via over-flights from an aircraft capable of moderately low flight altitude and able to drop small objects or a vessel of opportunity. This approach does require several of microbuoys, but fortunately they are usually comparably inexpensive. For the price of one $5k buoy that might survive one summer season, ten $500 microbuoys could be deployed, doubling the number of sensors present at any one time.

A potential scenario would involve routine drops along areas of high importance from Coast Guard domain awareness flights and ships of opportunity. Microbuoys measuring upper ocean heat content, sea state, or other parameters (depending on sensor configuration) would drift with surface currents for periods of approximately one month. Data would be available in near-real time from periodic uploads over satellite networks, for integration into ice and sea state prediction systems, reanalysis products, and scientific analysis. By having frequent deployments in an area, there is consistently one or more buoys in the location(s) of interest, something that cannot be guaranteed with a larger unmoored buoy. Microbouys could also play a role in field campaigns where deployment by hand is possible. For example, several microbuoys could be tossed into open sea-ice leads to monitor changes in ocean conditions during freeze-up or melt.

For the cases where a relative few measurements are needed (collecting no more than a few kB of data per day), microbuoys provide a cost-effective platform. They are well suited to taking advantage of existing traffic (aircraft or ship) for deployment, and offer significant flexibility in observing strategy through low unit cost. The Arctic Observing System of the future will take advantage of these types of instruments to supplement larger buoy systems in the rapidly changing environment.

References:

Bradley, Alice C, Scott Palo, Gabriel LoDolce, Doug Weibel, and Dale Lawrence. 2015. "Air Deployed Micro Buoy Measurement of Temperatures in the Marginal Ice Zone Upper Ocean during the MIZOPEX Campaign." *Journal of Atmospheric and Oceanic Technology*, March. American Meteorological Society. doi:10.1175/JTECH-D-14-00209.1.

Bradley, Alice C, Scott Palo, Christopher Zappa, Gabriel LoDolce, Doug Weibel, and Dale Lawrence. 2014. "Observations of Wind-Induced Motion in the Arctic Marginal Ice Zone." In *American Geophysical Union Fall Meeting*. San Francisco, CA.

Bradley, Alice C., Scott E. Palo, James Maslanik, G. LoDolce, D. Weibel, and D.A. Lawrence. 2014. "Wind-Driven Processes in the Surface Layer of the Marginal Ice Zone." In *44th International Arctic Workshop*. Boulder, Colorado.

Cassano, J.J., J.A. Maslanik, C.J. Zappa, A.L. Gordon, R. Cullather, and S.L. Knuth, 2010. "Wintertime observations of an Antarctic polynya with unmanned aircraft systems." In *Eos Trans.* AGU, vol. 91, p. 28, 2010.

Broadbent, Heather A, Stanislav Z Ivanov, and David P Fries. 2007. "A Miniature, Low Cost CTD System for Coastal Salinity Measurements." *Measurement Science and Technology* 18 (11): 3295–3302. doi:10.1088/0957-0233/18/11/005.

McGehee, David D, and Marshall D Earle. 2002. "Episodic Wave Data Capture With Miniaturized Instrumentation." In *OCEANS '02 MTS/IEEE*, 104–10.

Arctic Observing Summit (AOS)

Statement: The Arctic Biodiversity Data Service (ABDS)

Relevant to themes: 1-2

By: Tom Barry, CAFF Executive Secretary and Kári Fannar Lárusson, CAFF Secretariat

"Improve circumpolar cooperation in data gathering and assessment …" (Recommendation #10, Arctic Biodiversity Assessment: Summary for Policy Makers[a])

The Conservation of Arctic Flora and Fauna[b] (CAFF) is the biodiversity working group of the Arctic Council [c] and has a mandate to address the conservation of Arctic biodiversity, and to communicate its findings to the governments and residents of the Arctic, helping to promote practices which ensure the sustainability of the Arctic's living resources. It does so through various monitoring, assessment [d] and expert group [e] activities. CAFF's projects provide data for informed decision making to resolve challenges arising from trying to conserve the natural environment and permit regional growth. This work is based upon cooperation between all Arctic countries, Indigenous Organizations, international conventions and organizations.

CAFF released the Arctic Biodiversity Assessment [f] (ABA) a comprehensive report based on the best available scientific and traditional knowledge about the status and trends of Arctic biodiversity, included specific recommendations for action to address major pressures on biodiversity and knowledge gaps. In responding to ABA recommendation #10, CAFF has established the Arctic Biodiversity Data Service (ABDS www.abds.is). The ABDS is the data-management framework for information generated by projects and programs of CAFF. It is a publicly accessible, online, interoperable data management system that serves as a focal point and common platform for all CAFF programs and projects as well as a dynamic source for up-to-date circumpolar Arctic biodiversity information. The goal of the ABDS is to facilitate access, integration, analysis and reporting of biodiversity information for scientists, practitioners, managers, policy makers and others working to understand, conserve and manage the Arctic's wildlife and ecosystems. It works to ensure that biodiversity data are organised to guarantee a lasting legacy in a manner which facilitates:

- Data discovery and accessibility;
- Increased understanding;
- Informed and more rapid decision making;
- The widest possible exchange of relevant data;
- Highlight ongoing research; and
- Improve the visibility of the work of CAFF and its partners.

The ABDS is framework is constructed using GeoServer and GeoNetwork built over a PostgreSQL database - open source solutions designed to facilitate sharing of information.

ABDS cooperates with partners such as the Global Biodiversity Information Facility (GBIF), the Oceanic Biogeographic Information Systems (OBIS), the Polar Data Catalogue (PDC) and the Arctic Spatial Data Infrastructure (Arctic SDI) to work towards enhancing the quality and scope of information relating to Arctic biodiversity available to science and society. This includes increasing interoperability of data management frameworks, avoiding data duplication, applying common standards and processes for exchanging existing data, and for sharing future datasets.

For more information please visit: ABDS Website[g]; ABDS GeoNetwork[h]

---

[a] Conservation of Arctic Flora and Fauna (CAFF). 2013. Arctic Biodiversity Assessment: Report for Policy Makers. CAFF, Akureyri, Iceland. http://www.arcticbiodiversity.is/the-report/report-for-policy-makers

[b] http://www.caff.is/

[c] http://www.caff.is/arcticcouncil

[d] http://www.caff.is/assessments

[e] http://www.caff.is/expert-group

[f] http://www.caff.is/administrative-series/24-all-administrative-documents/293-actions-for-arctic-biodiversity-2013-2021-implementing-the-recommendations-of-th

[g] http://www.abds.is/

[h] http://geo.abds.is/geonetwork/srv/eng/catalog.search#/home

The Arctic Council's Arctic Adaptation Exchange Portal (AAEP): Where Arctic communities Share, Connect and Innovate for Resilient Responses to Environmental Change

Arctic communities possess a wealth of knowledge about landscape and ecosystem changes in their regions. This knowledge is an incredible resource that needs to be shared across the circumpolar North and beyond, to non-Arctic research and policy-making centers. The Arctic Adaptation Exchange Portal (AAEP), a project of the Arctic Council's Sustainable Development Working Group (SDWG) and The University of Alaska is supporting the flow of knowledge between Arctic communities for adaptive and resilient capacity that will enable us to respond to change in a way that is anticipatory rather than reactive. As an open and web-based platform, this information is also available for a range of other users, including researchers and policy-makers. A unique and distinguishing feature of the AAEP is that it is not geared primarily for scientists to use, recognizing the overwhelming number of databases and other technical sites that currently exist. Instead, the AAEP fills a current unmet niche: that of building a knowledge-base at ground level, where day to day adaptation actions are occurring right now, in real life and not theory.

To truly support the knowledge capacity that sustains resilient Arctic communities, the Arctic Adaptation Exchange Portal (AAEP) is expanding its existing platform to allow users to share innovations, problems, and solutions for resilient response to global and environmental change. Currently, the AAEP is a vibrant place to share research of all kinds across a variety of thematic and Arctic regional contexts. But the AAEP has the capacity to support and engage Arctic community members in a more dynamic role: through the Community Observation Network for Adaptation and Security (CONAS) and the joint Scandic-Russian community based observing effort, Snowchange the AAEP team, in partnership with residents, has identified 16 communities around the circumpolar region who are willing to participate in sharing their experiences of and solutions to arctic change. These include communities in the U.S., Russia, Norway, Sweden, and Finland. The AAEP continues to seek community partners across the circumpolar North.

Through an accessible web platform the planned re-design of AAEP serves as both information resource and climate change witness for Arctic communities. This re-design includes adding a user forum for frank discussion, and re-calibrating the AAEP "Explore" map. The map will be re-purposed to directly support community members who want to document their observations of tundra-level changes, and share local solutions to these changes.

With the new AAEP, users from Arctic communities can

- **share** resources and observations on a map. This allows users to document problems at specific locations arising from climate change, and also to share solutions. Shared resources can be in the form of documents, web pages, videos, or photos.
- **explore** problems and solutions of other Arctic communities. The AAEP provides Arctic communities with solution-finding tools to community problems that stem from climate change. These include the Arctic Water Resource Vulnerabilities Index (AWRVI).
- **connect** through an interactive forum for discussion, solution finding, and problem identification. These public forums are moderated and can be used for effective research and policy that is sourced from on-the-ground witnesses.
- **innovate** through discussion, observation, and solution-sharing.

Currently the Arctic Adaptation Exchange Portal unites 50+ Arctic & northern organizations supporting climate change and presents portal users with 900+ resources on Arctic climate change issues and solutions. These resources are submitted by AAEP curators and users, and are shared through the “Explore” circumpolar map. Included in these resources are Arctic datasets from the US Department of Interior (DoI).

History

The Arctic Adaptation Exchange portal is a project of the Arctic Council’s Sustainable Development Working Group. The AAEP began as a collaborative project between the University of Alaska Anchorage and the Government of Canada under the Canadian chairmanship of the Arctic Council. These groups, in partnership with Indigenous communities and government entities, built the AAEP in response to the need expressed by Arctic ministerial members at the 2011 Arctic Council Ministerial in Nuuk for stronger response to arctic-related adaptation. Nuuk delegates recognized a disconnect between the pace of academic research and the speed brought on by necessity for Arctic communities to developing response capacity. The current iteration of the Arctic Adaptation Exchange portal came out of a 2014 meeting with the Alaska EPSCoR AAEP Chair, U.S. and Canadian representatives.

In 2015 with the transfer of the Arctic Council chairmanship from Canada to the US, the University of Alaska took on the mantle of the Arctic Adaptation Exchange. Project co-leads within the Arctic Council’s Sustainable Development Working Group include the Government of Canada (Natural Resources Canada); the Climate Change Secretariat, Department of Environment, Government of Yukon; Aleut International Association; and Gwich’in Council International.

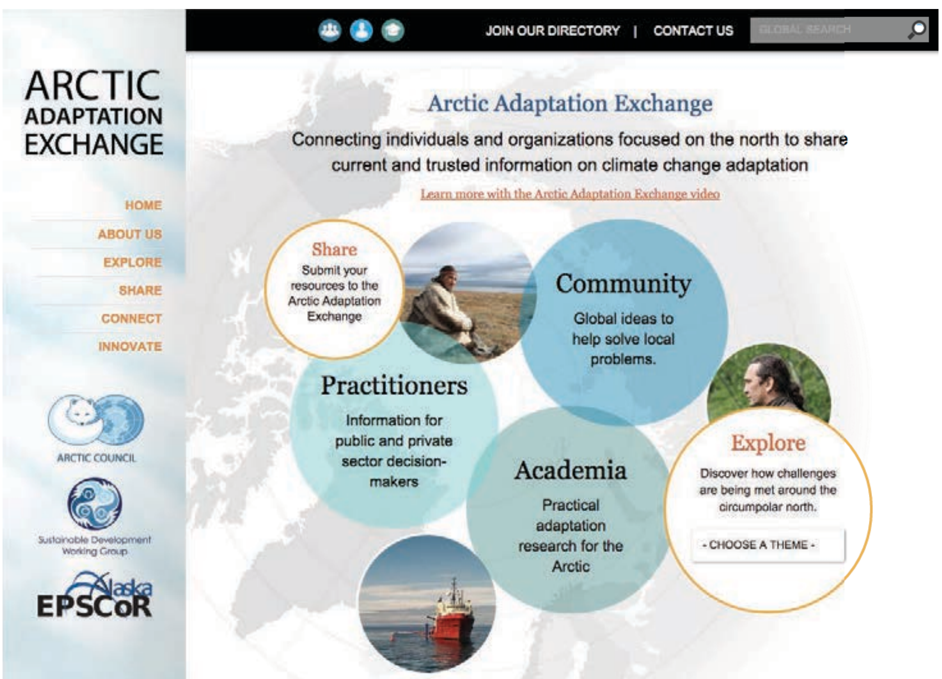

www.arcticadaptationexchange.com

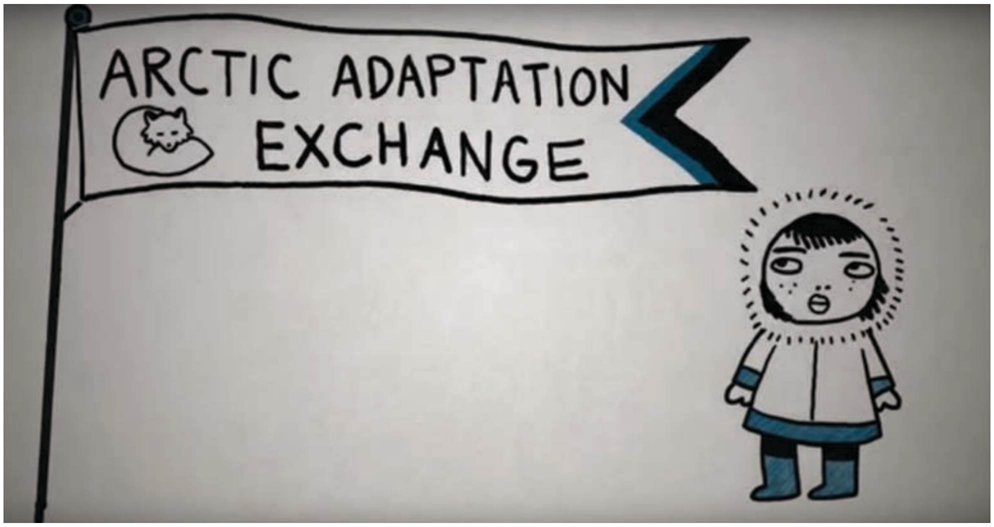

Arctic Adaptation Exchange video

A Pan-Arctic Airborne Sea Ice Observation System

S. Hendricks[1], C. Haas[2], S. Gerland[3], A. Herber[1], T. Krumpen[1], A. Mahoney[4], H. Eicken[4], R. Gerdes[1]

(1) Alfred-Wegener-Institut Helmholtz Zentrum für Polar und Meeresforschung, Bremerhaven, Germany

(2) York University, Earth & Space Science & Engineering, Toronto, Canada

(3) Norsk Polarinstitutt, Tromsø, Norway

(4) University of Alaska Fairbanks, Fairbanks, USA

Lead Author:

S .Hendricks, Alfred-Wegener-Institut Helmholtz Zentrum für Polar und Meeresforschung, Bremerhaven, Germany, Bussestr. 24, 27570 Bremerhaven, Germany, stefan.hendricks@awi.de

Theme 2: Technology and Innovation for sustained Arctic observations

Abstract

We present an Arctic sea-ice observation system that focuses on unique direct observations of sea ice plus snow thickness. A network of research institutions, the Alfred Wegener Institute, York University and the Norwegian Polar Institute, maintain an observation system that is embedded in several national and international projects and supported by research partners. Activities in the field include the use of long-range polar research aircraft and helicopter operations from research icebreakers and bases on land. Data collections are based on electromagnetic induction sounding and consistent time series are available in key regions of the Arctic Ocean since 2001. The increased use of polar research aircrafts in recent years has resulted in several initiatives that aim for long-term observations of ice thickness during seasonal minimum and maximum sea-ice extent in the Arctic. The scientific payload of the research aircraft of type Basler BT-67 and its capability to fly low-altitude surveys makes it an ideal tool for the validation and on-going verification of various satellite remote sensing products. The availability of airborne sea-ice thickness information spans the periods of different satellite sea-ice thickness retrieval concepts, such as the radar altimeters from Envisat and CryoSat-2 as well as the laser altimeter from ICESat-1 and -2. Wherever possible, the airborne surveys are accompanied by in-situ observations on the ice surface to compile a hierarchy of validation data from local to basin scales. Results of the observation network have found broad use for studying inter-annual variability and changes of sea ice thickness as well as the validation of satellite data products. We identify a gap of observations over the multi-year sea ice zone during the melt season and early freeze-up. We also stress the need for the continuation of a coordinated observational program that has produced a time series of sea ice thickness only paralleled by submarine observations. We plan to augment the observation system by simultaneous measurements of snow depth and to investigate opportunities for technological advances, such as the utilization of unmanned aerial systems.

Objective

Sea ice plays an important role in the polar and global climate system by controlling the surface energy balance and the interaction between atmosphere and oceans in high latitude. Therefore, the polar sea ice cover is a key indicator for the variability and changes of the polar climate system. The Global Climate Observation System (GCOS) selected sea ice as an Essential Climate Variable (ECV) and its observation is the objective of several national and international observation networks and initiatives. Key observation parameters are the extent, concentration and thickness of sea ice as well as the depth of the overlying snow layer and melt pond concentration in summer. The large and remote areas of ice-covered oceans with harsh environmental condition require the use of satellite remote sensing as an observational tool. The longest and continuous time series of Arctic sea ice are based on passive microwave datasets that can be utilized to derive sea ice extent and concentration at decadal scales. Recently, remote sensing products of sea ice thickness have emerged, a key physical parameter of the sea ice cover. The main challenges for sea ice thickness observations from space are the inter-annual variability and the significant seasonal cycle of ice surface conditions. One example is the lack of snow-depth data that may create significant errors of ice thickness retrievals from satellite freeboard measurements. The assessment of uncertainties in the sea ice mass budget through independent validation data sets therefore requires the presence of an observation system throughout the year.

The scale necessary to capture gradients of sea ice thickness and to provide meaningful sections of data for comparisons require either the use of long-range observation platforms, such as submarines or aircraft, or autonomous stations that can record sea ice parameters at a location for months and years. In addition, the need for consistency among data sets is an important factor for time series of high-resolution validation data sets that may bridge between several remote sensing mission concepts. One method that provides such datasets throughout different stages of developments of sea ice is airborne electromagnetic induction sounding (AEM). The underlying geophysical principle of electromagnetic induction sounding exploits the contrast of electrical conductivity between the sea ice and ocean layers. The method provides a profile of ice thickness that is smoothed by the size of the sensor footprint. Thus, maximum thicknesses at the deepest point of a pressure ridge are usually underestimated but comparisons to other methods demonstrate that the footprint smoothing is mass conserving. Hand-held or sled-mounted sensors for high-resolution measurements are in use as well, but airborne systems deliver long-range and high-resolution direct measurements of snow plus ice thickness (henceforth ice thickness) profiles that are only paralleled by submarine draft measurements.

Implementation

Several partners carry out AEM ice thickness measurements in the Arctic with simultaneous field work (Figure 1) throughout the year with the exception of the dark winter months with no-fly conditions. The Alfred Wegener Institute spearheaded the broad use of helicopter-towed AEM sensors for climate research with a pilot project in 2001 (Haas et al., 2009). The principal design is based on pioneering work dating back to several years earlier (Kovacs et al. 1987, Kovacs and Holladay, 1990). The so-called EM-Birds are rated as a standard external sling-load and can be used by several helicopter types with minimal preparation time. In practice, AEM systems can be deployed from research icebreakers, ice camps and airports nearby sea ice. This flexibility initiated several time series of AEM ice thickness in the Lincoln (Haas et al., 2010), Beaufort and Laptev Seas, Fram Strait (Renner et al., 2014; Krumpen et al. 2015) and the central Arctic. Technical advances and the use of research aircraft of the type Basler BT-67 opened the possibility for longer profiles with additional sensor equipment. The underlying principles require operations close to the ice surface in absence of conductive objects or electromagnetic sources in the very low signal frequency range. Though integration into the frame of an aircraft or helicopter have been implemented, towed systems have emerged as the commonly mode of operation for such measurements. Aircraft surveys therefore require operations at low altitudes to bring the sensor close to the ice-water interface where the bulk of the measured signal is generated. The additional scientific payload of these polar research aircraft leads to an efficient multi-purpose, multi-variable sea-ice observation platform that accommodates the need for different survey altitudes in the outgoing and return leg of the surveys, which have sufficient length due to the aircraft's operational range (Herber et al., 2012).

Today, an observational network building on various airborne assets operated by the Alfred Wegener Institute (AWI), York University (YU) and the Norwegian Polar Institute (NPI) acquires AEM ice thickness data. The observational strategy aims to assess sea ice conditions during the annual maximum ice extent in March/April, the melt season and the annual minimum in September. The field campaigns of all partners are closely tied to on-going satellite validation activities, such as the CryoSat-2 validation experiment (CryoVEx) or SMOS (SMOSice) as well as other observational programs, e.g. theSeasonal Ice Zone Observing Network (SIZONet), and the Transpolar System of the Arctic Ocean (Transdrift). In addition, we pursue other opportunities for cross-referencing and calibration such as with the U.S. Naval Research Laboratory's LiDaR surveys, NASA's IceBridge flights and the The Fram Strait Arctic Outflow Observatory. Field activities are funded either by national projects, international partnerships of participating research institutions or partners such as the European Space Agency (ESA). One example are repeated spring surveys since 2009 by aircraft of the AWI called Polar Airborne Measurements and Arctic Regional Climate Model Simulation Project (PAMARCMIP) that are supported financially and logistically by international partners like (Environment Canada, YU, University of Alaska Fairbanks through the U.S. National Science Foundation and industry and that tie into complementary observations such as those of SIZONet.

Activities

AWI operates two polar research aircraft (Polar-5 and Polar-6, see Figure 2) that are used for pan-Arctic measurements in spring ranging from the seasonal ice zone in the Beaufort/Chukchi Sea regions to the Greenland Sea and Fram Strait. In these campaigns, the aircraft are outfitted to serve multiple roles. The observation of ice thickness and morphology with an EM-Bird and scanning laser altimeter is carried out at low flight levels, while experiments on atmospheric chemistry and atmosphere-sea ice interaction on the same flights are carried out at higher altitudes. The conditions of the sea ice surface are documented with aerial photography (different automatized systems, single or stereo photography). In the melt season, the AWI observational program consists of aircraft surveys from Greenland (TIFAX: Thick Ice Feeding Arctic Export) and helicopter AEM measurements from the icebreakers R/V *Polarstern* (Germany). Here, measurements are complemented by aerial photography to document the coverage and evolution of melt ponds on the ice surface. YU operates a Basler BT-67 aircraft with an AEM system with a special regional focus in ice-covered regions of the Northwest Passage (Haas and Howell, 2015) and adjacent regions of the Canadian Archipelago in the Arctic Ocean. NPI implements AEM sea-ice thickness observations with a helicopter-based system, that operates from Norwegian research vessels (R/V *Lance*) or coast guard ships (KV *Svalbard*) with a regional focus in the Greenland Sea (Fram Strait), and Barents Seas, and the Arctic Basin north of Svalbard. Measurements are complemented with a stereo camera system. Norwegian Polar Institute's surveys are currently done every second or third year in the mentioned regions. Ship-borne activities by AWI and NPI generally include in-situ collection of sea ice parameters and the deployment of drifting buoys that measure time-series of sea ice parameters beyond the period of airborne surveys.

The activities are closely coordinated between the partners to sustain time series of sea-ice thickness in key regions and maximize temporal and spatial coverage. The results spawned several studies on changes of sea-ice thickness (e.g. Haas et al., 2010, Renner et al 2014, Lindsay and Schweiger 2015), the validation of satellite sea-ice thickness retrievals from altimetry and passive microwave missions (Laxon et al. 2013, Ricker et al 2014, Maaß et al. 2015, Kwok and Cunningham 2015, Tilling et al. 2015), the inter-calibration of different ice thickness retrieval methods (e.g. Mahoney et al, 2015), and exploration of inverse modeling approaches to determine optimal routing of measurement flights (Kaminski et al. 2015).

Outlook, Recommendations and Action Items

With the exception of one regular activity from Greenland between July and August, most of the long-range sea-ice thickness surveys by polar aircraft are carried out during spring. In summer instead, ship-borne activities become feasible that include the possibility to complete the observational hierarchy of local in-situ data collection, airborne measurement at mesoscale and satellite remote sensing data at basin scale. However, we identify a major gap in airborne surveys over the multi-year ice zone near the Canadian Archipelago during the melt season and early freeze-up; this region is mostly inaccessible to research icebreakers but represents an important part of the Arctic ice pack, including its role as a source of thick ice for the Beaufort and Chukchi Sea. This region requires additional attention and coverage. This recommendation is amplified by the need for validation of newly available monthly sea-ice thickness fields derived from the CryoSat-2 mission. Measurements during late summer or potentially early freeze-up have the potential to provide validation data for the CryoSat-2, Sentinel-3 and future ICESat-2 thickness fields early in the freezing season, at a time and location for which we are currently lacking validation data. Also, the lack of knowledge of the interannual variability of physical parameters that feed into satellite retrieval algorithms, such as snow depth or density, create the need for continued validation and verification by independent sea ice thickness information. Due to this reason, satellite products will not be able to supplant AEM measurements to a significant degree in the near future.

We therefore stress the need for the continuation and coordination of AEM sea ice thickness data acquisitions in the Arctic. AEM data provides consistent and direct observations of the ice thickness distribution that furnishes valuable information for the interpretation and validation of freeboard estimates from altimeters. As such it is the only data source other than increasingly scarce submarine data that provides profile measurements of the bulk of the total ice thickness, rather than a measurement of surface elevation or freeboard. Moreover, airborne platforms allow for the integration of a range of different measurements and instrumentation into a single airframe, fostering inter-disciplinary studies that are co-located in space and time. Through coordination among observing partners, including the use of buoys and satellite data to track ice, surveys can also be designed to allow repeat, semi-Lagrangian observations that will provide essential insight into the linkage between Arctic ice volume and dynamics. To better coordinate and support such flights, an international consortium that brings together operators, science users, private sector entities and others may help in the creation of a more robust, long-term program. Currently, not all parts of the surveys are rooted in long term funded programmes, which means that partners are depending on funding in new projects.

There is further opportunity to expand the observational network by coordinating with partners from China and Japan who also have the capability for airborne ice thickness measurements. Contributions by new partners are highly welcome since the current observation programme has a limited range of operations (see Figure 3 as an example for aircraft sea ice observations in spring). A particular lack of information exist in the Russian Arctic, mainly the Laptev and Kara Seas. The understanding of the processes that govern the inter-annual and long-term variability of sea ice thickness and extent needs measurements in these ice production regions. There is also a need to augment the capability of the observations system by simultaneous measurements of snow depth. Knowledge of snow depth is not only important for mass balance estimates from satellite remote sensing, but also as an input parameter for seasonal sea ice forecasts (Castro-Morales et al., 2014) in frameworks such as the Sea Ice Prediction Network.

While additional parameters such as snow depth will amplify the impact of the observing system for climate research, the core activity of AEM ice thickness surveys are becoming increasingly important for high-resolution, near-real-time regional studies in support of environmental assessments, ice navigation, and offshore engineering operations. Therefore, a key opportunity from the technology side is the development of AEM systems that lend themselves to deployment onboard unmanned aerial systems (UAS). As outlined above, such deployment faces key challenges with respect to miniaturization, reduction of noise and maintenance of data quality, but the potential rewards of such a system are high.

References

Castro-Morales, K., F. Kauker, M. Losch, S. Hendricks, K. Riemann-Campe and R. Gerdes (2014); Sensitivity to realistic ice thickness distribution sand snow parameterizations of simulated Arctic seaice, J. Geophys. Res., DOI: 10.1002/2013JC009342

Haas C., J. Lobach, S. Hendricks, L. Rabenstein, A. Pfaffling (2009): Helicopter-borne measurements of sea ice thickness, using small and lightweight, digital EM system. Journal of Applied Geophysics 03/2009; 67(3):234-241. DOI:10.1016/j.jappgeo.2008.05.005

Haas, C, Hendricks, S, Eicken, H, and Herber, A. (2010). Synoptic airborne thickness surveys reveal state of Arctic sea ice cover. Geophysical Research Letters, 37(09): L09501. doi: 10.1029/2010GL042652.

Haas, C., and S. E. L. Howell (2015), Ice thickness in the Northwest Passage, Geophys. Res. Lett., 42, 7673–7680, doi:10.1002/2015GL065704.

Hendricks S., P. Hunkeler, T. Krumpen, L. Rabenstein, H. Eicken, A. Mahoney (2014): Sea Ice Thickness Surveying with Airborne Electromagnetics - Grounded Ridges and Ice Shear Zones near Barrow Alaska. Arctic Technology Conference 2014, doi:10.4043/24552-MS

Herber, A., Haas, C., Stone, R., Bottenheim, J., Peter , L., Li, S., Staebler, R., Strapp, J. and Dethloff, K. (2012). Regular Airborne Surveys of Arctic Sea Ice and Atmosphere, EOS, Transactions, American Geophysical Union, 93 (4), pp. 41-42 .

Kaminski, T., F. Kauker, H. Eicken, M. Karcher (2014): Exploring the utility of quantitative network design in evaluating Arctic sea ice thickness sampling strategies. The Cryosphere, 9, 1721-1733, doi:10.5194/tc-9-1721-2015.

Kovacs, A., Holladay, J.S., 1990. Sea-ice thickness measurements using a small airborne electromagnetic sounding system. Geophysics 55, 1327–1337.

Kovacs, A., Valleau, N.C., Holladay, J.S., 1987. Airborne electromagnetic sounding of sea ice thickness and sub-ice bathymetry. Cold Regions Science and Technology 14, 289–311.

Krumpen, T., Gerdes, R., Haas, C., Hendricks, S., Herber, A., Selyuzhenok, V., Smedsrud, L., and Spreen, G.: Recent summer sea ice thickness surveys in the Fram Strait and associated volume fluxes, The Cryosphere Discuss., 9, 5171-5202, doi:10.5194/tcd-9-5171-2015, 2015

Kwok R., G. F. Cunningham (2015), Variability of Arctic sea ice thickness and volume from CryoSat-2, Phil. Trans. R. Soc. A 2015 373 20140157; DOI: 10.1098/rsta.2014.0157.

Laxon S. W., K. A. Giles, A. L. Ridout, D. J. Wingham, R. Willatt, R. Cullen, R. Kwok, A. Schweiger, J. Zhang, C. Haas, S. Hendricks, R. Krishfield, N. Kurtz, S. Farrell and M. Davidson (2013), CryoSat-2 estimates of Arctic sea ice thickness and volume, Geophys. Res. Lett., 40, 732–737, doi:10.1002/grl.50193

Lindsay, R. and Schweiger, A.: Arctic sea ice thickness loss determined using subsurface, aircraft, and satellite observations, The Cryosphere, 9, 269–283, doi: 10.5194/tc-9-269-2015, URL http://www.the-cryosphere.net/9/269/2015/, 2015.

Maaß N., L. Kaleschke, X. Tian-Kunze, M. Mäkynen, M. Drusch, T. Krumpen, S. Hendricks, M. Lensu, J. Haapala, C. Haas: Validation of SMOS sea ice thickness retrieval in the northern Baltic Sea. 02/2015; 67. DOI:10.3402/tellusa.v67.24617

Mahoney A.R., Hajo Eicken, Yasushi Fukamachi, H. Ohshima, D. Shimizu, Chandra Kambhamettu, R. MV, Stefan Hendricks, Joshua Jones: Taking a Look at Both Sides of the Ice: Comparison of Ice Thickness and Drift Speed as

Observed from Moored, Airborne and Shore-Based Instruments Near Barrow, Alaska.. Annals of Glaciology 01/2015; 56(69):363-372. DOI:10.3189/2015AoG69A56

Renner, A.H.H., Gerland, S., Haas, C., Spreen, G., Beckers, J.F., Hansen, E., Nicolaus, M., Goodwin, H. 2014. Evidence of Arctic sea ice thinning from direct observations. Geophysical Research Letters 41(14): 5029–5036. DOI:10.1002/2014GL060369

Ricker, R., Hendricks, S., Helm, V., Skourup, H., and Davidson, M.: Sensitivity of CryoSat-2 Arctic sea-ice freeboard and thickness on radar-waveform interpretation, The Cryosphere, 8, 1607–1622, doi: 10.5194/tc-8-1607-2014, URL http://www.the-cryosphere.net/8/1607/2014/, 2014.

Tilling Rachel L., Andy Ridout, Andrew Shepherd, Duncan J. Wingham (2015), Increased Arctic sea ice volume after anomalously low melting in 2013, Nature Geoscience 8, 643–646, doi:10.1038/ngeo2489

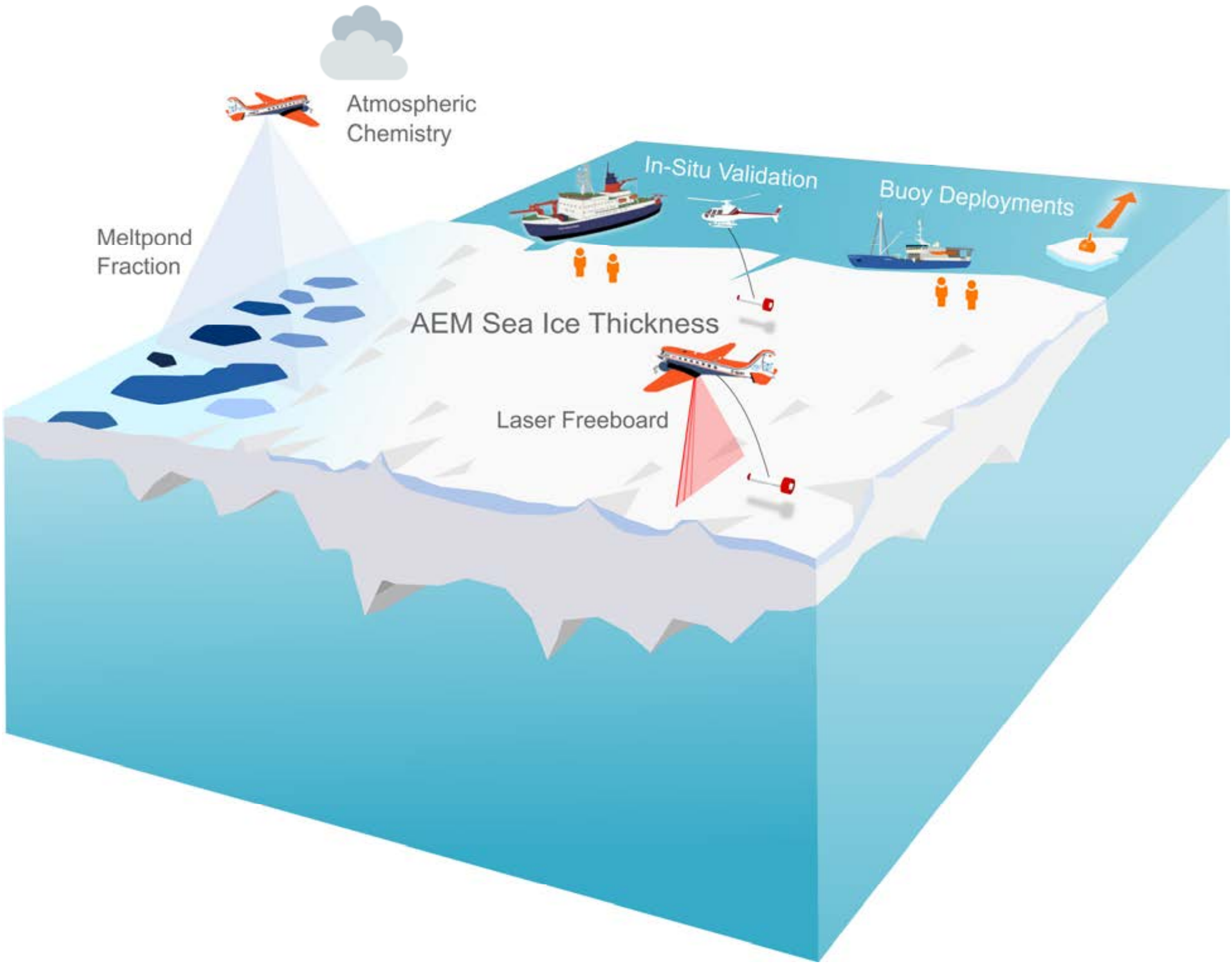

Figure 1: Schematic of a comprehensive Sea Ice Observation System with a focus on direct observations of sea-ice thickness with airborne electromagnetic induction sounding (AEM). Research aircraft and helicopters are frequently used to tow AEM sensors from early spring to late autumn in the Arctic. The scientific payload of research aircraft allows multi-role science missions that include observation of atmospheric and other parameters for the validation of satellite remote-sensing products. Coincident and high-resolution in-situ observations are available by activities that are based on research icebreakers including the deployment of drifting buoys to fill data gaps between airborne observations.

Figure 2: Polar-5, a polar research aircraft of the Alfred Wegener Institute outfitted with an AEM sensor for direct sea-ice thickness observations. York University operates are similar aircraft of the same model and scientific payload.

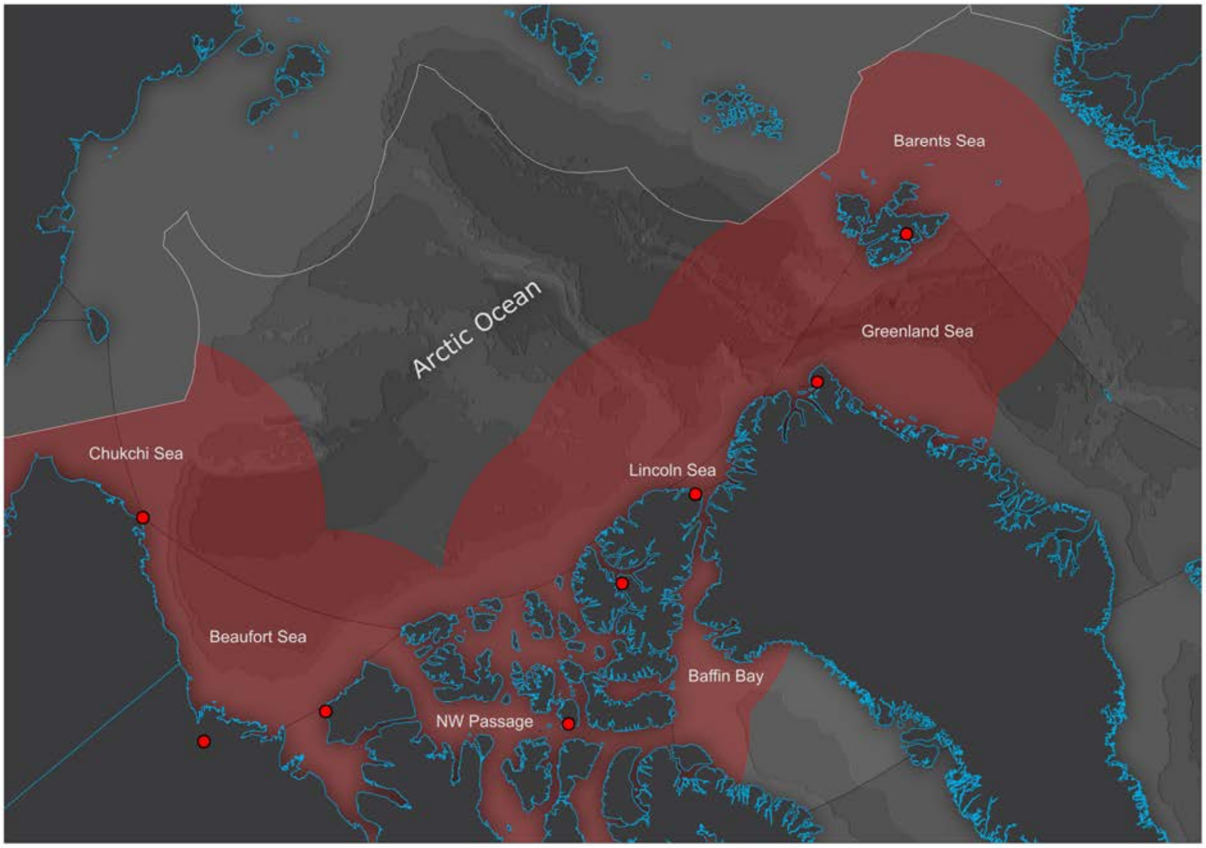

Figure 3: Current operational coverage of the sea ice observation system by polar research aircraft for sea-ice thickness surveys from logistic hubs (red dots) in the western Arctic.

Abstract Title

Exploring the Arctic: Integrating Earth Observations on the WorldView Discrete Global Grid System

Authors

Joanne Jones, PYXIS, Anchorage Alaska

Perry Peterson, PYXIS, Kingston, Ontario

Abstract Text

Humanity's ability to measure, monitor, and communicate over the vastness of the entire Earth is unprecedented. Trends point to ever growing volumes of rich data describing the planet. People, from scientist to citizens, expect this information in a form that can answer their pressing questions…instantly. At the same time, we are experiencing the rapid unprecedented consequences of environmental changes. It is hoped that the data and information describing these changes can be transformed into the knowledge and decisions that will mitigate the cost.

Nowhere are these changes more evident than in the Arctic. The singularity of a pole in a region of vying national interests, climate change, resource extraction, emerging shipping routes, and a suffering ecosystem have given the Arctic new attention. However, access to Arctic geospatial data has long been a challenge. Remoteness and equatorial fixated map projections have made it difficult to include polar data in the normal offerings of scientific and consumer mapping products. Timely decisions are further hampered by the conventional GIS approach where data must be pre-integrated by expert analysts before it can produce answers and insight to pressing geospatial questions. Arctic projected webmaps provide anticipated stop gap but fail to produce the robustness of a system that can answer unanticipated questions.

The Open Geospatial Consortium (OGC) has recently introduced a new Earth reference standard that promises to solve these challenges. It is formally called a Discrete Global Grid System (DGGS) and is analogous to any discrete "Digital" data structure - as opposed to the continuous "Analog" model of the Earth represented by geographic coordinates. OGC defines a DGGS as: *"a spatial reference system that uses a hierarchical tessellation of cells to partition and address the globe. DGGS are characterized by the properties of their cell structure, geo-encoding, quantization strategy and associated mathematical functions."*

Essentially, a DGGS is a spatial reference that uses equal area cells to partition and address the entire globe. Each tiny cell – they can be infinitesimally small - has a unique address similar to the cells of a spreadsheet. The hierarchy of cells provide rapid aggregation and decomposition of data necessary for online access and transmission speeds. As a global spatial reference system, Polar data in a DGGS is accurately portrayed and equally integrated with any map information of the world. Geospatial data values from any source, type, format, spatial reference, spatial scale, or frequency can be held in a DGGS. With the trend to more open on-demand systems, DGGS provide a user centric approach where end-users can search and explore for interesting data from multiple content providers simultaneously. Answering complex geospatial questions in the form

of “Where is it?” and “What is here?” are simple set theory operations. Big Earth Data that is aligned to a DGGS is easy to access, store, sort, process, transmit, integrate, visualize, analyse and model.

PYXIS WorldView DGGS has been shown to fulfill a vision for a web enabled Digital Earth that is so simple to use that children can effectively understand facts and events that define the condition and history of our planet. WorldView allows multiple data sources to be integrated and analyzed in one workflow without the need to convert or change spatial reference systems. WorldView DGGS permits easy repeatable manipulation, visualization and analysis of measurements from any location at any scale. The rapid search, discovery, and combing of geospatial content across multiple data jurisdictions has been successfully demonstrated using the WorldView DGGS in many OGC testbeds and Global Earth Observation System of Systems (GEOSS) pilot projects.

Visualization of complex analysis can be an effective method of influencing a multitude of policy and decision making processes which impact Arctic issues. A DGGS can be a major advancement in the understanding of the Arctic environment where data can be accurately represented with minimal distortion. Users can easily access and combine data to problem solve and make decisions concerning issues in the Arctic in a timely manner. Access to large scale Arctic data sources that can be viewed geospatially is a common process shared between scientists, engineers, teachers, and citizens.

The new OGC DGGS standard provides the basis for adopting this new digital Earth approach to geospatial decision-making. WorldView demonstrates that a DGGS is a simple solution for data integration, visualization and analysis. The authors will present use cases that exemplify how WorldView DGGS supports easy access to large and complex Arctic geospatial datasets to perform analysis, on one platform, in one workflow.

Keywords

Digital Earth Reference Model, Discrete Global Grid System, OGC, Arctic, Geographic Information Systems (GIS), Spatial Analysis, Earth Observations, Polar Projections